On the Feasibility of RTapp™ as a Daily Delivered Dose Evaluation Tool for Adaptive Lung Stereotactic Body Radiation Therapy (SBRT)

A THESIS

SUBMITTED TO THE FACULTY OF MEDICAL PHYSICS GRADUATE

PROGRAM UNIVERSITY OF MINNESOTA

BY

Nur Izzati Huda Zulkarnain

IN PARTIAL FULFILLMENT OF THE REQUIREMENTS FOR THE DEGREE OF

MASTER OF SCIENCE

Yoichi Watanabe, advisor

Damien Mathew, co-advisor

31 August 2020

Acknowledgments

I wish to express my sincere appreciation to Dr. Yoichi Watanabe and Dr. Damien Mathew for their kindness and patience in providing valuable and constructive advice. Without their guidance, the goal of this project would not have been realized. I want to acknowledge the support of ©SegAna LLC for the opportunity, especially Dr. Anand Santhanam, Saty Seshan, and Dan Elliott, for their assistance throughout this project. I would also like to thank Dr. L. Chinsoo Cho for his help in target delineation, which is crucial in this project, and Dr. Kevin Leder for his willingness to become one of the graduation committee members.

Many thanks to all the faculty, staff, and fellow students in the Medical Physics Graduate Program and Department of Radiation Oncology for their support and help throughout my two years at the University of Minnesota. I am also exceptionally grateful for the scholarship support from the Ministry of Education Malaysia. Last but not least, nothing would have been possible without the love and nurturing of my parents, family members, friends, and loved ones. To Farhah Fakhira Azli, whom I lost on 21 July 2011, this is for you.

Abstract

Purpose: RTapp™ is a daily dose evaluation software developed by ©SegAna LLC. It utilizes deformable image registration (DIR) to recontour structures and evaluate the dose delivered in every fraction. The program updates patient anatomy based on daily cone-beam CT and assesses the dose distribution according to the detected changes. RTapp™ can be a useful tool in lung stereotactic body radiation therapy (SBRT) to avoid underdosing target and overdosing organs at risk (OARs). In this study, the feasibility of RTapp™ to assess the quality of treatment delivered in every fraction was investigated.

Methods: 20 lung SBRT patients were retrospectively analyzed with RTapp™. For each patient, the simulation CT images, treatment structures, plan, and dose from Pinnacle^3 treatment planning system, daily CBCT from MOSAIQ record and verify system, and pre-treatment couch alignment information from Varian on-board imaging (OBI) software were imported into the RTapp™ software. Bidirectional DIR was applied to update the planning target volumes and OARs and the dose distribution to the patient's daily anatomy. The ability of RTapp™ to deform structures and update dose was validated. The deformed RTapp™ ITV (rtITV) was compared to physician-drawn ITV (pITV). Dice coefficient (DC) and Hausdorff distance (HD) were used to analyze the overlap and similarity of the two structures in 3D Slicer. The accuracy of dose calculations by RTapp™ was evaluated by recalculating the doses with Pinnacle^3 for the target coverage and several dose metrics to lungs, heart, cord, esophagus, and airway.

Results: Ten, three, and one out of 20 patients showed more than 5% decrease in PTV $V_{100\%}$, PTV $V_{90\%}$, and both ITV $V_{100\%}$ and GTV $V_{100\%}$, respectively. Five patients were selected to validate RTapp™'s ability to deform structures and dose. The mean (± standard deviation) values of the Dice coefficient ranged from 0.75 to 0.81, with a mean of 0.78 ± 0.03, indicating good agreements

between the rtITV and pITV. Meanwhile, the average, 95%, and maximum HD had mean values (± standard deviation) 1.44 ± 0.27 mm, 3.61 ±0.62 mm and 6.14 ± 1.24 mm respectively. The difference in the PTV coverage had the largest variation. Difference in PTV $V_{100\%}$ and PTV $V_{90\%}$ have variance values of 42.41% and 8.89% respectively, compared to ITV $V_{100\%}$ and GTV $V_{100\%}$ with variance of 3.67% and 0.88% respectively. 97% of the fractions had the ITV and GTV coverage difference within ± 2.5%. The difference in the dose to OARs was the highest in regions with a steep dose gradient, specifically, the dose to lungs.

Conclusion: The ability of RTapp™ as a daily dose evaluation tool to maintain the quality of lung SBRT treatment was validated. The fast auto-segmentation and dose distribution updates according to daily anatomical changes provided by the RTapp™ software is highly beneficial as a step towards the realization of adaptive radiation therapy without introducing time and resource constraints. However, further studies are necessary to validate the accuracy of RTapp™ DIR for clinical applications.

Table of Contents

List of Tables

List of Figures

List of Abbreviations

SBRT – Stereotactic body radiation therapy

CT – Computed tomography

GTV – Gross tumor volume

OAR – Organ-at-risk

MIP – Maximum intensity projection

4DCT – Four-dimensional CT

ITV – Internal target volume

PTV – Planning target volume

CBCT – Cone-beam CT

HU – Hounsfield units

DIR – Deformable image registration

DVF – Deformable vector field

RTOG – Radiation Therapy Oncology Group

DVH – Dose-volume histograms

TPS – Treatment planning system

DICOM – Digital Imaging and Communications in Medicine

SRO – Spatial registration object

pITV – Physician-drawn ITV

rtITV – RTapp™ deformed ITV

DC – Dice coefficient

HD – Hausdorff Distance

COM – Center of mass

1. Introduction

1.1. Lung stereotactic body radiation therapy

Lung stereotactic body radiation therapy (SBRT) is a hypofractionated radiotherapy procedure. Compared to conventional radiotherapy, higher doses per fraction are delivered in fewer fractions. The radiobiological endpoint of SBRT is better tumor control with lower normal tissue toxicity. To achieve such a goal, SBRT requires highly conformal dose distributions and a sharp decrease in dose gradients outside of targets. These are achieved by precise volume delineation, motion management, and accurate tumor localization with the guidance of advanced imaging procedures and rigorous treatment planning methods[1,2,3].

Computed tomography (CT) is the primary procedure to acquire simulation images for clear visualization of the targets and patient anatomy. The gross tumor volume (GTV) and organs-at-risk (OARs), which include the esophagus, trachea, bronchi, spinal cord, and heart, are outlined according to clinically approved protocols. Maximum intensity projection (MIP) images derived from four-dimensional CT (4DCT) can provide more information on internal target volume (ITV) by accounting for intrafraction target motion due to respiration and cardiac function[4,5]. Also, an abdominal compression device is used during CT simulation and treatment to suppress target motion, enabling a reduction of the size of target margins[6,7].

The integration of advanced imaging procedures, motion management, and tumor localization in SBRT enables a smaller margin, thus a relatively tighter planning target volume (PTV). SBRT treatment planning aims to optimize dose metrics to the PTV and OARs by delivering a conformed high dose to targets with sharp isotropic dose fall-off and minimizing the dose spillage to normal tissues. This optimization is achieved by using ten or more coplanar or

non-coplanar beams. Prescription dose is directed to a lower isodose line, between 60% to 90% dose, which results in the maximum dose occurring within the PTV[4,7,8]. Prescription dose, the number of fractions, and treatment planning criteria are determined according to respective lung SBRT protocols.

The position during simulation CT is reproduced in the course of treatment. The combination of image-guided patient positioning and motion management devices is of paramount importance to minimize intra- and inter-fraction position errors. In addition to laser-based alignment, cone-beam CT (CBCT) is used to perform more reliable and precise patient positioning, especially in lung SBRT, where target visualization is needed for precise target positioning[7,9]. Immobilization devices such as chest compression, body frame, and vacuum cushion are effective in reducing the patient's motion during treatment and minimize respiratory motion[6,10,11]. These localization methods also ensure the reproducibility of patient position in every fraction.

1.2. Daily dose evaluation

Radiation therapy treatment is generally delivered with the assumption that the anatomy of the patient remains the same as the simulation CT. However, anatomical changes due to the change in tumor volume, the position shift of the structures due to organ filling or emptying, or patient weight loss might occur during treatment. These anatomical changes may result in geometric and dose variations, which can compromise target coverage and OAR doses when suitable plan modifications are not done[12]. The intra- and inter-fraction geometric and dose variations are minor in lung SBRT due to the smaller number of fractions and strict motion management[13]. However, compared to conventional therapy, the volume of the target is smaller, and the dose delivered per fraction is larger. Hence, if any geometric or dose variations are not detected, significant

underdosing of target or dose spillage to OARs might occur[14]. Consequently, the daily changes of the tumor position and size in lung SBRT necessitate performing daily dose evaluation[15,16,17,18].

Daily dose evaluation is advantageous to detect plans that exceed tolerance guidelines and identify the need for plan adaptation. It leverages daily acquired images, mainly the readily available CBCT, to update anatomical and dosimetric information. Although it is inferior to that of the planning CT, the soft-tissue contrast and spatial resolution of CBCT is adequate for target and structure delineation and can be used for volume tracking throughout the treatment[19,20]. Also, the dose calculated on CBCT can be used by comparing it with the plan dose. The dose calculation requires a Hounsfield unit (HU)-to-density table calibrated to the CBCT modality and the contours of structures to consider any anatomical changes[21,22,23]. However, manual structure segmentation is a challenge to implement daily dose evaluation due to time requirements, an increase in workload, and interobserver variability.

Deformable image registration (DIR) distorts voxels of a moving image to align it with a reference image. The magnitude and direction of the distortion are defined as the deformable vector field (DVF)[24]. It can mitigate the limitations of manual delineation by utilizing DVF to map the original planning structures to the deformed images[25]. DIR can also be used to estimate dose accumulation by deforming dose grids and to integrate the deformed dose in each treatment fractions[26,27]. By employing CBCT and DIR for daily dose evaluation, the applicability of the original treatment plan to the new condition can be evaluated for the dosimetry consistency and accuracy.

1.3. RTapp™

RTapp™ is a daily dose evaluation software developed by ©SegAna LLC (Orlando, FL). It can be used as a tool to assess the quality of daily treatment delivery. The software uses treatment plan information and daily treatment images to visualize anatomy variations in every fraction and analyze whether the change will cause out-of-tolerance dosimetric constraints. Treatment constraints are evaluated by comparing the achieved constraint values against recommended values in the Radiation Therapy Oncology Group (RTOG) protocols and values approved during treatment planning.

RTapp™ performs daily dose evaluation using the treatment plan, dose, structures, registration information, and CBCT images. By processing the daily data, users can evaluate if patient realignment or daily anatomy changes will result in suboptimal treatments. It will mark a plan with "REVIEW" if the achieved quantities exceed 5% difference from plan values or "NOT MET" if constraints exceed RTOG recommended values. The percent difference can be changed to a more lenient or stricter threshold. Figure 1.1 shows the RTapp™ interface. Users can simultaneously view the planning and treatment images, examine dose-volume histograms (DVH) of structures, and analyze the dose trend of each structure to make clinical decisions accordingly[28].

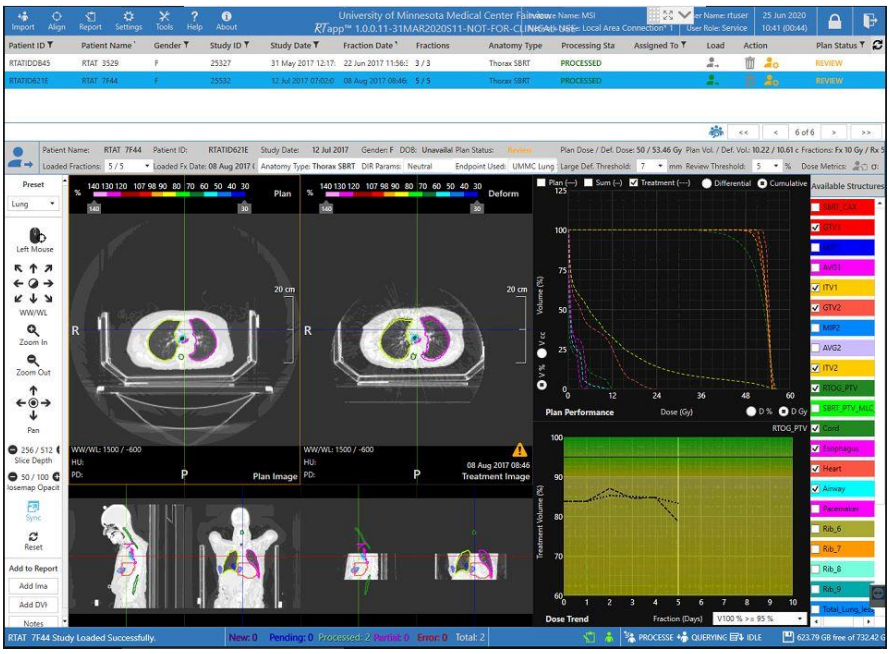

Figure 1.1: RTapp™ main interface. Users are equipped with tools for importing, aligning images, generating a report, and anonymizing a study in the top toolbar. The planning image and treatment image are shown side by side, and both planning and updated structures displayed simultaneously in the treatment image panel.

A prominent aspect of RTapp™ is the implementation of DIR algorithms to provide fast structure recontouring and update the dose to target and OARs[29]. The intensity-based DIR algorithm calculates the degree of image similarity by matching anatomical areas with similar pixel values. It occurs in both directions, registering the planning image to the treatment image and vice versa. The DVF obtained from the bi-directional DIR is used to deform planning structures and dose distribution. The deformed dose is displayed in the treatment image. RTapp™ updates the dose to the deformed structures and enables analysis of both daily dose and estimation of accumulated dose to the current fraction. RTapp™ also predicts when the treatment plans will become out-of-tolerance.

1.4. Aims

In this study, the feasibility of RTapp™ for lung SBRT was investigated by validating RTapp™'s DIR capability to deform the planning structures and dose.

1) The deformed ITVs were compared with physician-drawn ITVs by using DIR metrics, Dice coefficient and Hausdorff distance, which analyze the overlapping and dissimilarities of the structures, respectively.
2) Once the reliability of RTapp™'s DIR is established, the updated dose distributions were compared to the dose calculated in the Pinnacle^3 treatment planning system. The comparison was made between RTapp™ and Pinnacle^3 for the dose metrics as per RTOG 0813 protocol for GTV, ITV, PTV, lungs, heart, cord, esophagus, and airway.

2. Methods and Materials

2.1. Patients

Twenty patients with non-small cell lung cancer, who underwent lung SBRT treatment, were selected. The planning CT images were taken with a Phillips Brilliance Big Bore CT simulator (Phillips, Amsterdam, Netherlands). Elekta body frame with chest compression plate (Elekta, Stockholm, Sweden) and Civco Vac-Lok vacuum cushion (CIVCO Medical Solutions, Orange City, IA) were used for immobilization of patients during the CT simulation and SBRT treatments. The SBRT treatment was planned with a Pinnacle^3 treatment planning system (TPS) (Philips Radiation Oncology Systems, Fitchburg, WI). The dose specification and dose-volume limits to critical organs followed the RTOG 0813 guideline. The prescription dose of 45-54 Gy was delivered to an isodose level of 80% to 90% in three or five fractions. Patients were treated on Varian TrueBeam linear accelerator (Varian Medical Systems, Palo Alto, CA) equipped with onboard CBCT imager. Daily CBCT images were acquired for treatment positioning. The data of the daily couch shifts for isocenter alignment were saved in the MOSAIQ software (Elekta, Stockholm, Sweden).

Figure 2.1 summarizes the process to analyze the feasibility of RTapp™ as a daily dose evaluation tool. The ability of RTapp™ DIR algorithm to propagate contours and update dose needs to be confirmed to establish confidence in the reported treatment plan evaluation. The target volumes are compared against physician-drawn target volumes, while the updated dose calculation results are compared against Pinnacle^3 dose calculation. The methods to compare both structures and doses will be discussed in sections 2.3 and 2.4, respectively.

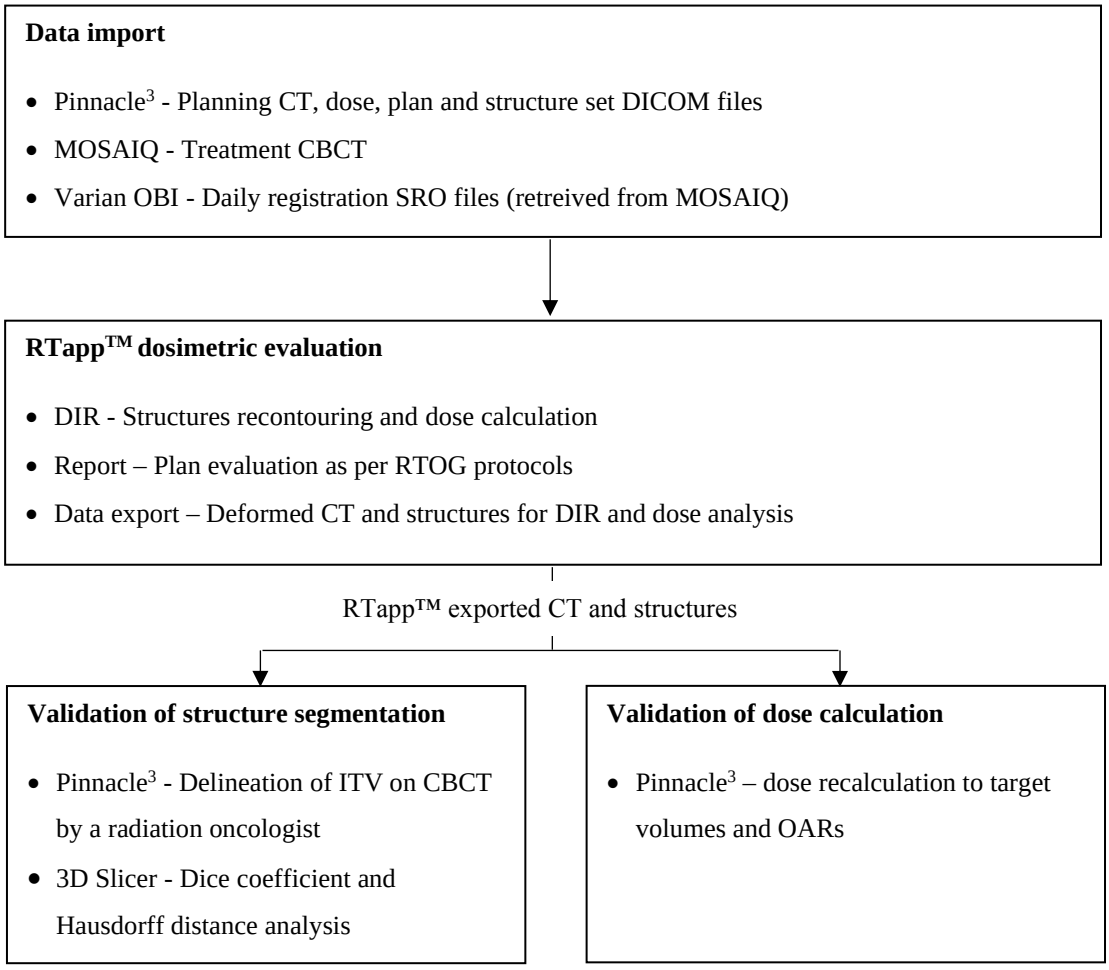

Figure 2.1. Workflow to analyze the feasibility of RTapp™

2.2. RTapp™ dosimetric evaluation

Digital Imaging and Communications in Medicine (DICOM) files of planning CT and CBCT images, structure set, dose, and plan, and spatial registration object (SRO) files containing alignment information were imported for processing in RTapp™. The anatomy type (Thorax SBRT), and lung SBRT dose metric, and structures were selected upon data retrieval on RTapp™. Table 2.1 shows the structures and UMMC dose metrics chosen for the treatment plans. RTapp™ reports contain the plan, achieved, and accumulated constraint values. RTapp™ allows the selection of a DIR parameter related to the bias of the algorithm in detecting deformation. The

Conservative parameter makes it less likely for the algorithm to identify a displaced voxel while selecting Aggressive makes the algorithm more sensitive to displaced voxel. The nominal choice, Neutral DIR parameter, was used to process all 20 patients.

Table 2.1. List of structures and their corresponding dose metric analyzed in RTapp™.

Structures	Dose metric
GTV	$V_{100\%} \geq 99\%$
ITV	$V_{100\%} \geq 99\%$
RTOG PTV	$V_{100\%} \geq 95\%$, $V90_{\%} \geq 99\%$
Left and right lungs	$D_{1500cc} \leq 12.5$ Gy, $D_{1000cc} \leq 13.5$Gy
Heart	$D_{15cc} \leq 32$ Gy
Cord	$D_{0.25cc} \leq 22.5$ Gy, $D_{0.5cc} \leq 13.5$ Gy,
Esophagus	$D_{5cc} \leq 27.5$ Gy
Airway	$D_{4cc} \leq 18$ Gy

2.3. Validation of the structure segmentation algorithm of RTapp™

An experienced radiation oncologist delineated the ITV (pITV) on all CBCT for five selected plans. The volumes of pITV and RTapp™ deformed ITV (rtITV) were computed in Pinnacle[3]. The similarity of pITV and rtITV was analyzed in the free open-source software, 3D Slicer, by analyzing the geometric-based DIR metrics: Dice coefficient (DC) and Hausdorff distance (HD)[30]. Both DIR metrics are widely used to evaluate the performance of the deformed image registration[31,32,33,34,35]. Rigid registration was used to align the deformed CT to the daily CBCT via the "Transforms" module in 3D Slicer. The centers of mass (COM) of the two ITVs

were aligned by minimizing the distance between the two COMs. The coordinates of COMs, (x,y,z), of the two ITVs were identified in Segment Comparison of the "Radiotherapy" module. The x-, y- and z- axes correspond to left-right, anterior-posterior, and inferior-superior directions. Translations in these three directions were equal to the difference between the points x, y, and z, respectively, of the two ITVs.

Note that DC indicates the degree of overlapping between rtITV and pITV. DC is a measure of the similarity of the automatically generated rtITV to the reference pITV[36,37]. It is given by,

$$DC = \frac{2|rtITV \cap pITV|}{|rtITV| + |pITV|}$$

where DC of zero indicates no overlapping, and conversely, DC of unity indicates perfect overlapping[38].

Meanwhile, HD calculates the maximum distance between the two closest neighboring points of the segmentations. It is sensitive to outliers, which is valuable to detect a large segmentation error[39,40]. It is given by,

$$h(rtITV, pITV) = \max_{a \in rtITV} \min_{b \in pITV} \|a - b\|$$

where *h* is the directed Hausdorff distance. It is the maximum distance for all points *a* to the closest point *b*. Three types of Hausdorff distances were computed in this study: average HD, 95% HD, and maximum HD[41]. Average HD is the average of *h(rtITV,pITV)* and *h(pITV,rtITV)*, while 95% HD is *h* greater or equal to exactly 95% of the other points. The max HD is the maximum of the two *h* and is also known as the undirected Hausdorff distance, given by

$$H(rtITV, pITV) = \max\left(\left(h(rtITV, pITV), h(rtITV, pITV)\right)\right).$$

Figure 2.2 shows a representation of DC and HD when comparing two structures. Average HD is HD averaged overall points and is less sensitive to the outlier, overall.

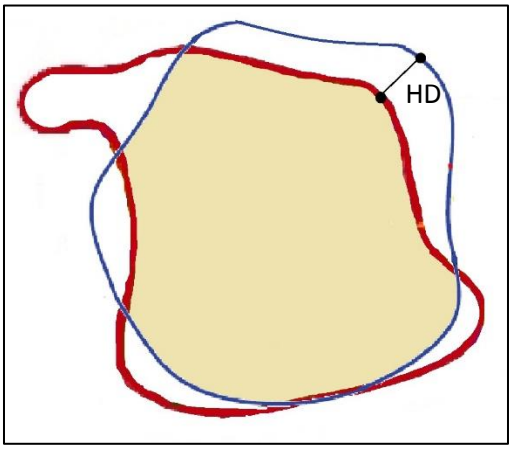

Figure 2.2. The shaded area corresponds to the overlapping of the structures, while HD indicates the Hausdorff distance between two points of the structures.

2.4. Validation of RTapp™ dose calculation algorithm

RTapp™ deformed CT and structures were exported to Pinnacle[3] for dose calculation. We used the Dynamic Planning module of Pinnacle[3] for the analysis[42]. The module automatically applied rigid registration to align the planning CT images to the deformed CT images. The dose prescriptions and beam setups used for treatment plans were applied to the RTapp™ deformed CT and the structure set. Manual adjustments of treatment isocenter and/or GTV were made to ensure the treatment isocenter is at the GTV's center of mass. Table 2.2 lists the compared dose metrics to validate the accuracy of the dose calculations of RTapp™.

Additionally, the dose metrics given in Table 2.1 were compared to validate the treatment objectives evaluated by RTapp™ against the objectives calculated in Pinnacle[3]. Furthermore, the difference in volumes that received specific doses was compared.

Table 2.2. Dose metrics used to validate dosimetric results in RTapp™ against the dose metrics calculated in TPS.

Structures	Dose metrics
GTV	$V_{100\%}$
ITV	$V_{100\%}$
RTOG PTV	$V_{100\%}$, $V_{90\%}$
Left and right lungs	D_{1500cc}, $D_{1000cc,}$ $V_{2.6Gy}$
Heart	D_{15cc}, $V_{6.4Gy,}$
Cord	$D_{0.25cc}$, $D_{0.5cc}$ $V_{4.5Gy,}$
Esophagus	D_{5cc}, $V_{5.5Gy,}$
Airway	D_{4cc}, $V_{3.6Gy,}$

3. Results

3.1. RTapp™ dosimetric evaluation

3.1.1. Target coverage

Figure 3.1 displays a report generated by RTapp™ that shows the patient information, plan details, and dose metrics. The results of processed structures are shaded blue. Table 3.1 summarizes the differences between the target coverage of the plan and the target coverage estimated by RTapp™ after treatment. Positive values indicate an overestimation of RTapp™ estimated target coverage. Ten patients showed a decrease of more than 5% in PTV $V_{100\%}$. The PTV $V_{90\%}$ value of three patients decreased by more than 5%. Only one patient showed a decrease of more than 5% in both ITV and GTV $V_{100\%}$. Figure 3.2 shows the RTapp^{TM} results for all five fractions of three patients. RTapp^{TM} suggested that the PTV $V_{90\%}$ of RTAT 3529 and the PTV $_{V90\%}$, ITV $V_{100\%}$, and GTV $V_{100\%}$ of RTAT 74FD already decreased by more than 5% at the first fraction. On the other hand, the PTV $V_{90\%}$ of RTAT 20B8 was not compromised until the third fraction.

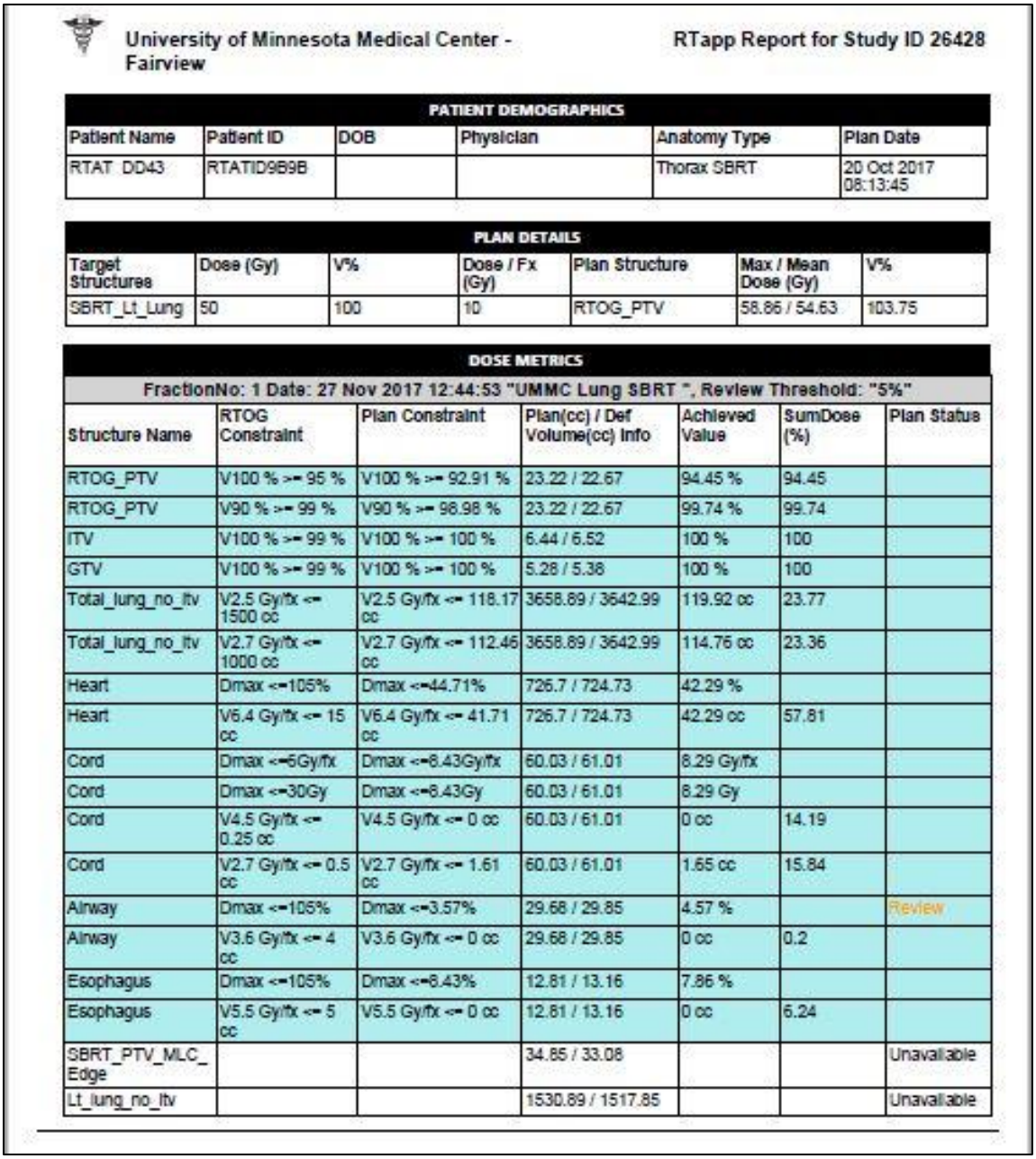

University of Minnesota Medical Center - Fairview

RTapp Report for Study ID 26428

PATIENT DEMOGRAPHICS

Patient Name	Patient ID	DOB	Physician	Anatomy Type	Plan Date
RTAT_DD43	RTATID9B9B			Thorax SBRT	20 Oct 2017 08:13:45

PLAN DETAILS

Target Structures	Dose (Gy)	V%	Dose / Fx (Gy)	Plan Structure	Max / Mean Dose (Gy)	V%
SBRT_Lt_Lung	50	100	10	RTOG_PTV	58.86 / 54.63	103.75

DOSE METRICS

FractionNo: 1 Date: 27 Nov 2017 12:44:53 "UMMC Lung SBRT ", Review Threshold: "5%"

Structure Name	RTOG Constraint	Plan Constraint	Plan(cc) / Def Volume(cc) Info	Achieved Value	SumDose (%)	Plan Status
RTOG_PTV	V100 % >= 95 %	V100 % >= 92.91 %	23.22 / 22.67	94.45 %	94.45	
RTOG_PTV	V90 % >= 99 %	V90 % >= 98.98 %	23.22 / 22.67	99.74 %	99.74	
ITV	V100 % >= 99 %	V100 % >= 100 %	6.44 / 6.52	100 %	100	
GTV	V100 % >= 99 %	V100 % >= 100 %	5.28 / 5.38	100 %	100	
Total_lung_no_itv	V2.5 Gy/fx <= 1500 cc	V2.5 Gy/fx <= 118.17 cc	3658.89 / 3642.99	119.92 cc	23.77	
Total_lung_no_itv	V2.7 Gy/fx <= 1000 cc	V2.7 Gy/fx <= 112.46 cc	3658.89 / 3642.99	114.76 cc	23.36	
Heart	Dmax <=105%	Dmax <=44.71%	726.7 / 724.73	42.29 %		
Heart	V6.4 Gy/fx <= 15 cc	V6.4 Gy/fx <= 41.71 cc	726.7 / 724.73	42.29 cc	57.81	
Cord	Dmax <=6Gy/fx	Dmax <=8.43Gy/fx	60.03 / 61.01	8.29 Gy/fx		
Cord	Dmax <=30Gy	Dmax <=8.43Gy	60.03 / 61.01	8.29 Gy		
Cord	V4.5 Gy/fx <= 0.25 cc	V4.5 Gy/fx <= 0 cc	60.03 / 61.01	0 cc	14.19	
Cord	V2.7 Gy/fx <= 0.5 cc	V2.7 Gy/fx <= 1.61 cc	60.03 / 61.01	1.65 cc	15.84	
Airway	Dmax <=105%	Dmax <=3.57%	29.68 / 29.85	4.57 %		Review
Airway	V3.6 Gy/fx <= 4 cc	V3.6 Gy/fx <= 0 cc	29.68 / 29.85	0 cc	0.2	
Esophagus	Dmax <=105%	Dmax <=8.43%	12.81 / 13.16	7.86 %		
Esophagus	V5.5 Gy/fx <= 5 cc	V5.5 Gy/fx <= 0 cc	12.81 / 13.16	0 cc	6.24	
SBRT_PTV_MLC_Edge			34.85 / 33.08			Unavailable
Lt_lung_no_itv			1530.89 / 1517.85			Unavailable

Figure 3.1: The first page of the report generated by RTapp™. The dosimetric analysis of the selected structures are shaded blue, and the plan Status is flagged "REVIEW" for D_{max} to airway because the achieved value exceeds the plan value.

Table 3.1. Plan prescriptions and differences of target coverage: PTV $V_{100\%}$ and $V_{90\%}$, ITV $V_{100\%,}$ and GTV $V_{100\%}$ of the treatment plan and RTapp™ (at the completion of treatment).

Patient	Plan dose (Gy)	Number of fractions	Isodose line	ΔPTV $V_{100\%}$ (%)	ΔPTV $V_{90\%}$ (%)	ΔITV $V_{100\%}$ (%)	ΔGTV $V_{100\%}$ (%)
RTAT A561	54	3	90	-4.65	-1.23	-0.09	0
RTAT 2AC4	50	5	80	-3.01	-0.49	0	0
RTAT 267D	50	5	90	-4.1	-2.45	-1.46	-0.51
RTAT 20B8	50	5	79	-12.1	-5.62	0	0
RTAT 3529	54	3	85	2.16	-6.02	-3.22	-2.45
RTAT 716F	54	3	87	-6.97	-2.8	-1.8	-0.46
RTAT 74FE	50	5	85	-8.67	-3.89	-0.91	-0.91
RTAT 8C16	50	5	80	0.94	0.15	0	0
RTAT 7F44	50	5	92	-7.07	-1.78	0	0
RTAT 2EC9	45	5	90	-5.57	-0.8	-0.28	-0.07
RTAT 882B	54	3	90	-5.81	-3.06	-0.16	0
RTAT E83F	50	5	85	-8.83	-1.36	-0.09	0
RTAT DD43	50	5	85	1.2	0.07	0	0
RTAT 74FD	40	5	90	-9.69	-8.29	-7.21	-5.34
RTAT AF8F	50	5	80	-2.36	-0.46	-0.38	-0.41
RTAT 3E47	54	3	83	-6.47	-1.8	0	0
RTAT 2CA2	50	5	80	-0.8	-0.28	0	0
RTAT C7CB	50	5	81	-3.54	-0.26	0	0
RTAT FB7C	50	5	80	-3.62	-0.35	0	0
RTAT 9F44	54	3	80	-10.95	-4.16	0	0

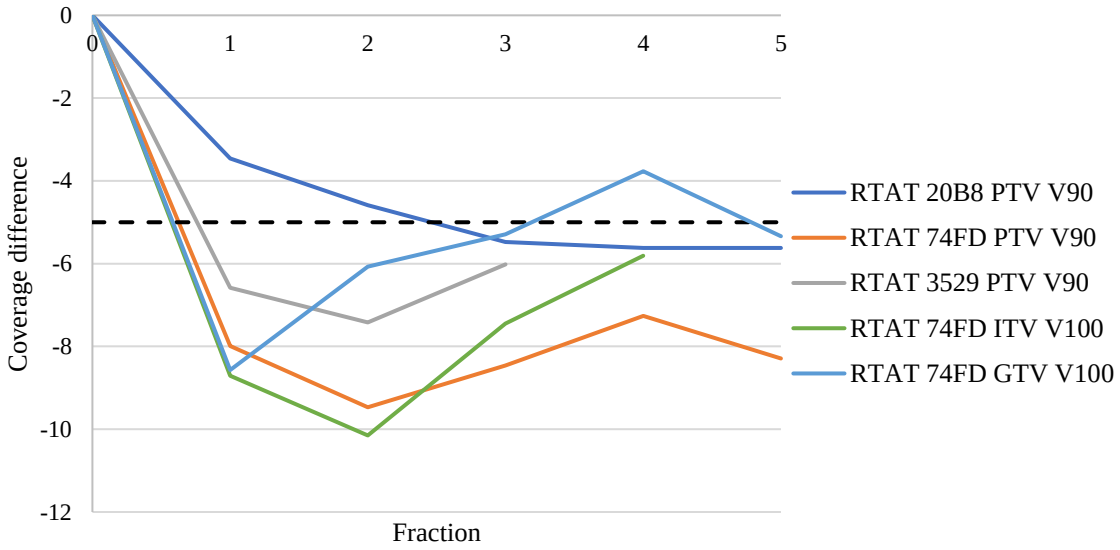

Figure 3.2. Coverage difference between treatment plan and RTapp™ predictions at the end of every fraction for three patients. The dashed line represents the tolerance value of -5% difference.

Figure 3.3 summarizes the dose metric of OARs listed in Table 2.1 for all patients. At every fraction, RTapp™ predicted the treatment dose, which is the dose at treatment completion accounting for the anatomical conditions on that fraction and assuming if the conditions persist to the end of the treatment course. All predicted treatment-completion dose to OARs did not exceed RTOG 0813 recommended values given in Table 2.1. The mean, median, and standard deviation of the differences between planning and treatment OAR dose metrics are shown in Table 3.2. The doses to the lungs, heart, and the 0.25 cc of the cord showed an increase at the treatment completion, while the doses to the esophagus, airway, and the 0.5 cc of the cord decreased. Figure 3.4 summarized the difference between the planning dose to OARs and the predicted dose to OARs at the treatment completion for every fraction.

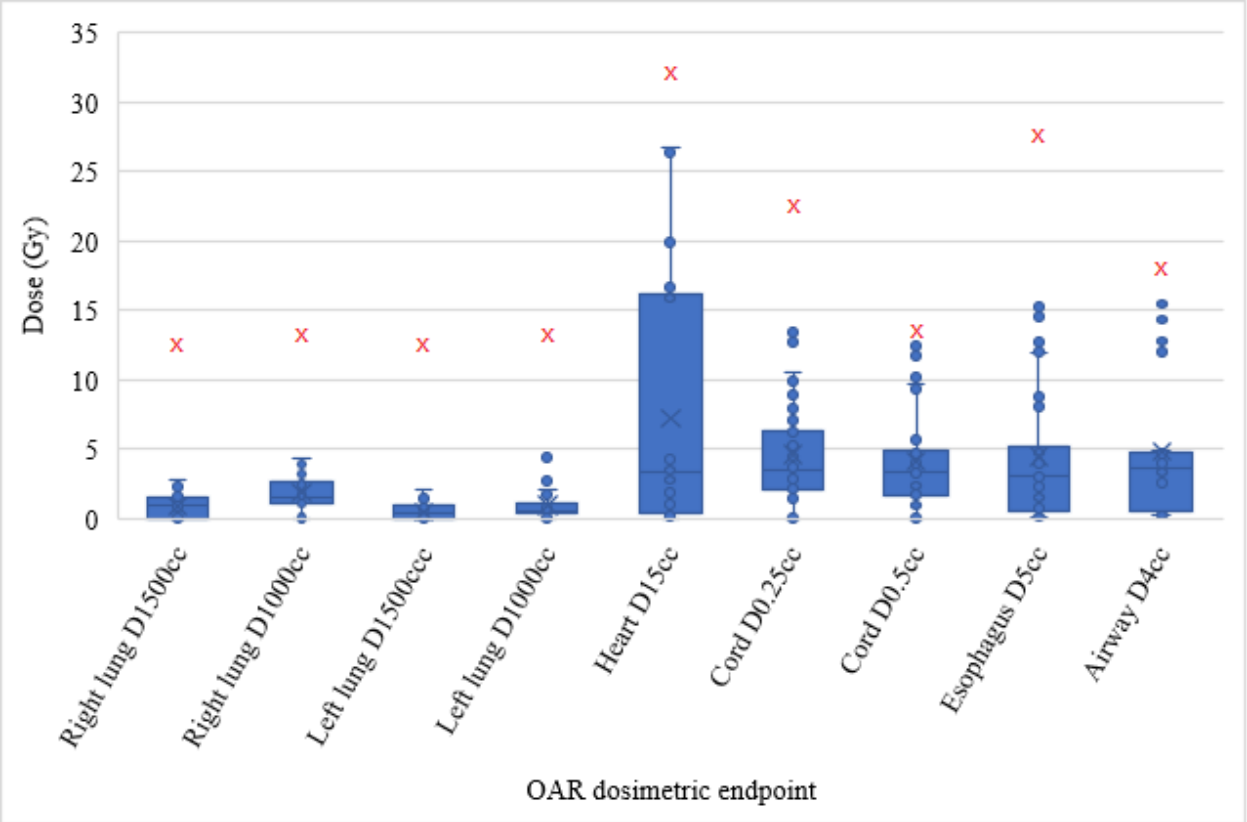

Figure 3.3. Predicted dose to the critical volume of OARs at treatment completion for every fraction based on RTOG 0813. The red crosses indicate the maximum dose to the critical volumes.

Table 3.2. Mean, median, and standard deviation of the difference between dose metrics to OAR at treatment completion compared to planning doses.

Dose metric	Mean	Median	Standard deviation
Right lung D_{1500cc} (Gy)	0.69	0.72	0.22
Right lung D_{1000cc} (Gy)	1.02	1.04	0.32
Left lung D_{1500cc} (Gy)	0.46	0.34	0.24
Left lung D_{1000cc} (Gy)	0.78	0.44	1.54
Heart D_{15cc} (Gy)	0.46	0.32	0.25
Cord $D_{0.25cc}$ (Gy)	0.43	0.54	0.54

Cord $D_{0.5cc}$ (Gy)	-0.04	-0.04	0.32
Esophagus D_{5cc} (Gy)	-0.21	-0.09	0.25
Airway D_{4cc} (Gy)	-0.04	0.01	0.27

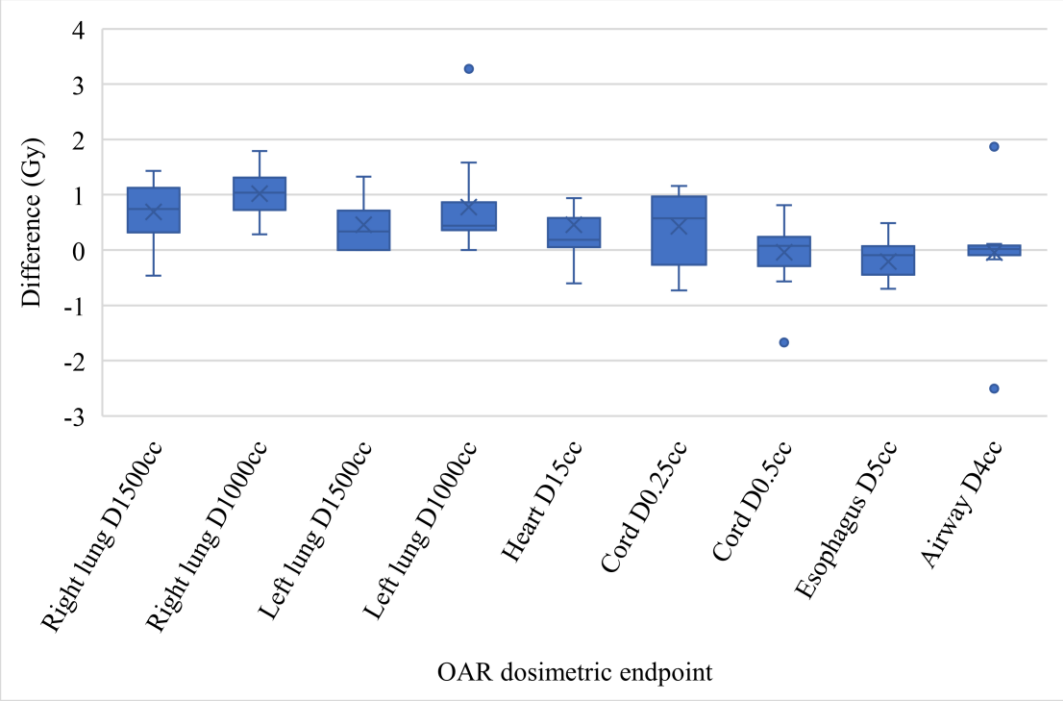

Figure 3.4. Difference between planning OAR dose metrics to treatment dose metrics predicted in RTapp™

3.1.2: Target volumes

Tables 3.3, 3.4, and 3.5 compile the difference between RTapp™-predicted and planning PTV, ITV, and GTV, respectively. Figures 3.5 and 3.6 show the relationship between the relative volume difference given by $\frac{Volume_{RTapp}-Volume_{plan}}{Volume_{plan}}$ and the difference of metrics PTV $V_{100\%}$, PTV $V_{90\%}$, ITV $V_{100\%}$ and GTV $V_{100\%}$.

Figures 3.5 and 3.6 show that the relative volume differences of PTV, ITV, and GTV were positive for most cases. This means that RTapp™ often provided larger target volumes than the

plan volume. The metric differences were negative when the relative volume difference of PTV was positive. But, when the relative volume difference of PTV was negative, the metric difference values were either positive or negative. On the other hand, the metric differences of ITV and GTV were always negative, indicating the ITV and GTV coverages were consistently underestimated by RTapp^{TM} regardless of the amount and direction of volume change.

From Figure 3.6, we found a weak negative correlation between volume difference with ITV $V_{100\%}$ and GTV $V_{100\%}$ (r = -0.18 for both metrics). However, Figure 3.5 shows that there is a stronger correlation with PTV $V_{100\%}$ and PTV $V_{90\%}$ (r = -0.62 and -0.38, respectively). This correlation implies that RTapp™ predicts lower target coverage when the target volume increases. However, RTAT 3529 shows decreasing tumor volume throughout the treatment, but this case was predicted to have an underdosing of PTV $V_{90\%}$. This implies that it is not sufficient to predict the underdosing of target volume solely by observing the dynamic change of tumor volume. RTapp™ prevents this overlook by estimating the dose accumulation in every fraction.

Table 3.3. The planning PTV and difference between the planning PTV and RTapp™ predicted PTV in every fraction.

Patient	Planning PTV	PTV volume difference (cc)				
	(cc)	Fx 1	Fx 2	Fx 3	Fx 4	Fx 5
RTAT A561	14.67	0.28	0.38	1.14	-	-
RTAT 2AC4	29.01	2.57	3.02	2.26	2.4	1.83
RTAT 267D	45.93	0	4.52	2.28	4.17	3.16
RTAT 20B8	7.95	0.49	0.52	0.77	0.75	0.98
RTAT 3529	12.85	-1.07	-0.88	-0.54	-	-
RTAT 716F	12.52	1.28	0.88	2.05	-	-
RTAT 74FE	43.83	3.92	13.11	6.51	4.41	7.03

RTAT 8C16	12.25	-0.35	-0.38	-0.57	-0.06	-0.19
RTAT 7F44	68.47	-1.12	3.8	2.63	2.65	3.27
RTAT 2EC9	36.05	1.98	3.5	1.88	-1.58	-2.26
RTAT 882B	28.6	3.36	3.07	3.8	-	-
RTAT E83F	15.78	1.53	2.09	2.82	1.98	1.91
RTAT DD43	23.22	-0.55	-0.67	-0.89	-0.86	0.87
RTAT 74FD	29.95	3.7	5.33	3.92	4.06	2.77
RTAT AF8F	7.68	0.14	0.65	0.39	0.45	0.87
RTAT 3E47	8.32	0.65	1.41	0.87	-	-
RTAT 2CA2	11.65	0.06	0.25	0.11	-0.09	0.01
RTAT C7CB	13.7	0.73	1.23	1.58	0.35	1.02
RTAT FB7C	15.26	-0.8	0.41	0.74	0.32	0.76
RTAT 9F44	8.43	0.06	0.94	0.34	-	-

Table 3.4. The planning ITV and difference between the planning ITV and RTapp™ predicted ITV in every fraction.

Patient	Planning ITV (cc)	ITV volume difference (cc)				
		Fx 1	Fx 2	Fx 3	Fx 4	Fx 5
RTAT A561	2.71	-0.05	-0.04	-0.04	-	-
RTAT 2AC4	8.7	0.36	1.11	0.88	0.5	0.36
RTAT 267D	16.28	0	1.42	0.4	0.82	0.53
RTAT 20B8	1.09	0.12	0.07	0.1	0.1	0.1
RTAT 3529	2.35	-0.22	-0.21	-0.02	-	-
RTAT 716F	1.97	0.36	0.24	0.45	-	-
RTAT 74FE	14.09	1.12	4.72	3.45	1.86	3.56
RTAT 8C16	1.9	-0.16	-0.09	-0.18	-0.05	-0.06

RTAT 7F44	24.07	2.21	2.25	1.73	1.8	1.1
RTAT 2EC9	18.84	1.58	2.65	1.36	-1.6	-2.24
RTAT 882B	3.21	0.38	0.57	0.38	-	-
RTAT E83F	2.84	0.69	0.93	0.94	1.06	1.01
RTAT DD43	6.44	0.08	0.51	0.22	0.53	0.85
RTAT 74FD	8.81	1.44	2.06	1.78	1.46	1.21
RTAT AF8F	1.35	0.07	0.19	0.16	0.1	0.23
RTAT 3E47	1.07	0.14	0.27	0.15	-	-
RTAT 2CA2	2.45	-0.02	-0.04	0.03	-0.07	0.02
RTAT C7CB	2.64	0.23	0.39	0.54	0.16	0.12
RTAT FB7C	2.6	-0.12	0.11	0.18	0	0.09
RTAT 9F44	1.15	0.12	0.25	0.18	-	-

Table 3.5. The planning GTV and difference between the planning GTV and RTapp™ predicted GTV in every fraction.

Patient	Planning GTV (cc)	GTV Volume difference (cc)				
		Fx 1	Fx 2	Fx 3	Fx 4	Fx 5
RTAT A561	1.77	-0.03	-0.02	-0.11	-	-
RTAT 2AC4	5.2	0.3	0.71	0.59	0.2	0.27
RTAT 267D	12.39	0	1.09	0.39	0.78	0.5
RTAT 20B8	0.68	0.09	0.02	0.04	0.05	0.06
RTAT 3529	1.18	-0.1	-0.1	-0.02	-	-
RTAT 716F	1.39	0.31	0.15	0.34	-	-
RTAT 74FE	14.07	1.13	4.61	3.45	1.86	3.56
RTAT 8C16	1.34	-0.08	-0.05	-0.09	-0.01	0.01
RTAT 7F44	10.79	1.43	1.4	1.19	1.11	0.42

RTAT 2EC9	15.47	1.44	2.57	1.43	-1.53	-2.11
RTAT 882B	1.21	0.05	0.13	0.09	-	-
RTAT E83F	1.78	0.57	0.73	0.69	0.85	0.78
RTAT DD43	5.28	0.1	0.53	0.29	0.58	0.82
RTAT 74FD	5.22	1.19	1.46	1.53	1.06	0.93
RTAT AF8F	1.24	0.05	0.17	0.17	0.09	0.21
RTAT 3E47	0.71	0.1	0.18	0.09	-	-
RTAT 2CA2	1.29	0.01	-0.02	0.04	-0.04	0.01
RTAT C7CB	2.17	0.19	0.34	0.44	0.14	0.11
RTAT FB7C	1.17	-0.07	-0.04	0.09	-0.02	-0.01
RTAT 9F44	0.71	0.1	0.2	0.16	-	-

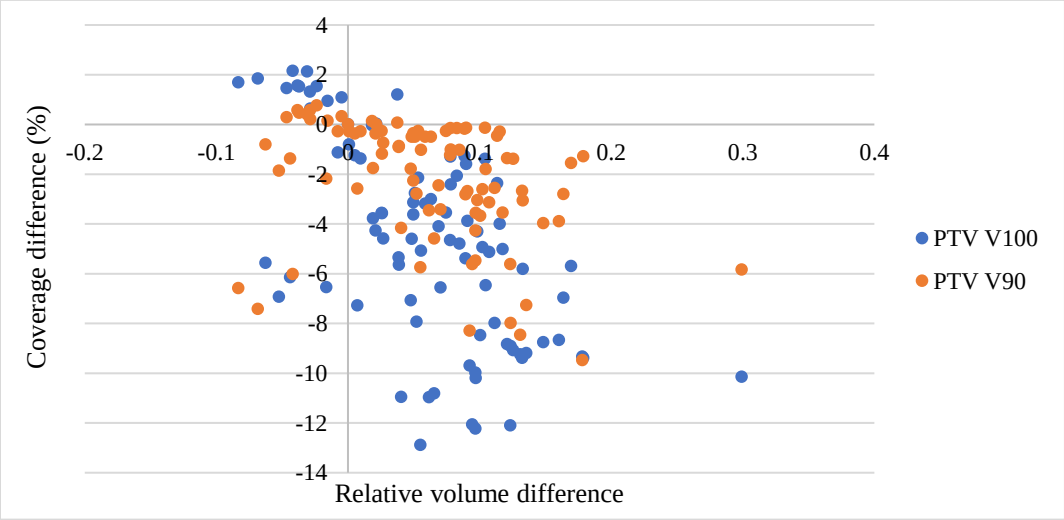

Figure 3.5. Relationship between planning and RTapp™ PTV $V_{100\%}$ and PTV $V_{90\%}$ difference with relative PTV volume difference.

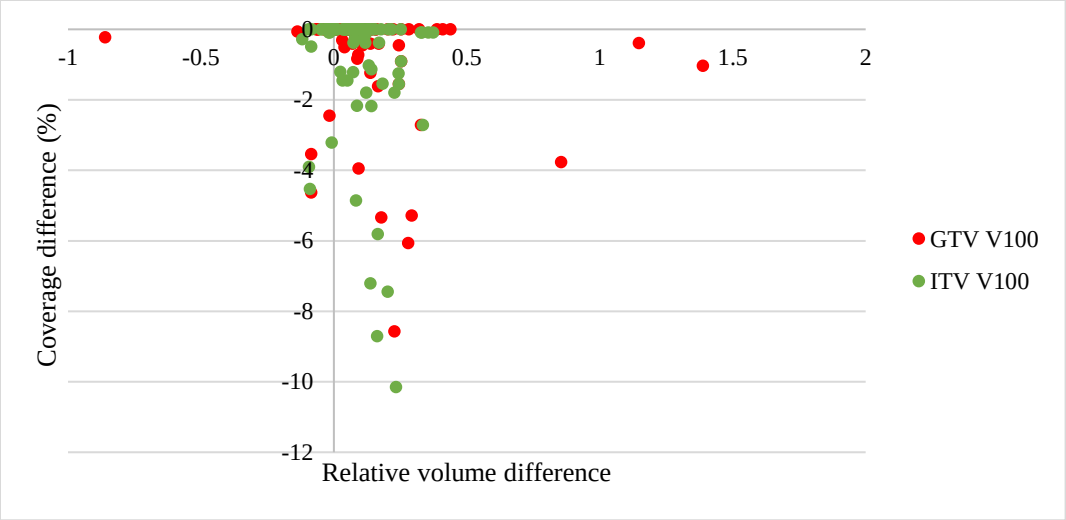

Figure 3.6. Relationship between planning and RTapp™ ITV $V_{100\%}$ and GTV $V_{100\%}$ difference with relative ITV and GTV volume difference.

3.2 Validation of the structure segmentation algorithm of RTapp™

Figure 3.7 shows the correlation between the RTapp™ estimated ITV (rtITV) to the physician-drawn ITV (pITV). Two of the five cases in the graph, RTAT 20B8 and RTAT 74FD, were identified in section 3.1 to have compromised PTV $V_{90\%}$ and ITV $V_{100\%}$ at the completion of treatment. The volumes of these cases are smaller than the other three cases on the graph. Figure 3.8 shows the rtITV and pITV for all five fractions. As seen in Figure 3.7, the rtITV highly correlated with their corresponding pITV ($r = 0.96$); however, Figure 3.8 indicates that the interfraction volume trend of rtITV and pITV did not agree with each other. For example, the volume of pITV of RTAT 267D decreased after fraction 3, but the volume of rtITV shows no significant decrease in the same fractions.

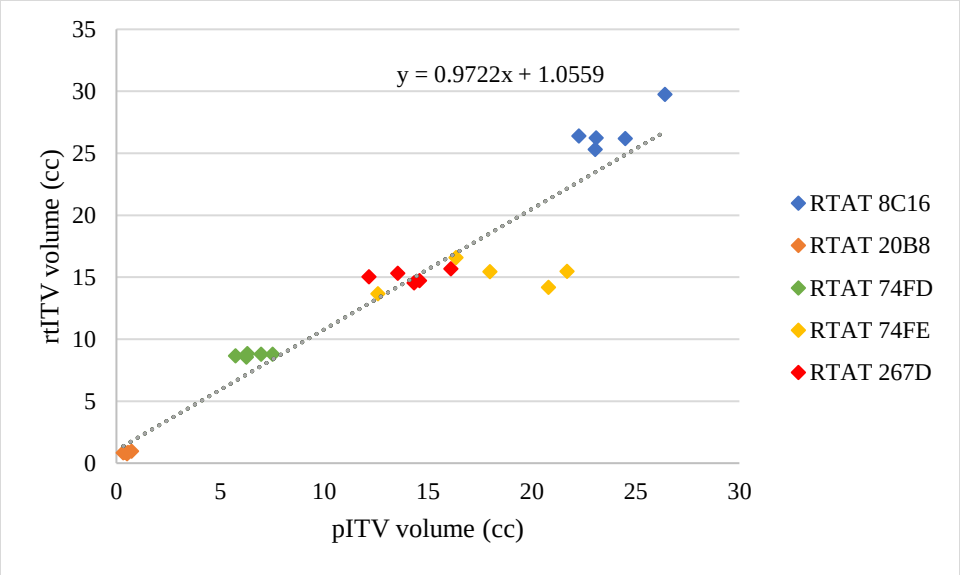

Figure 3.7: Correlation between volumes of rtITV and pITV for five selected cases.

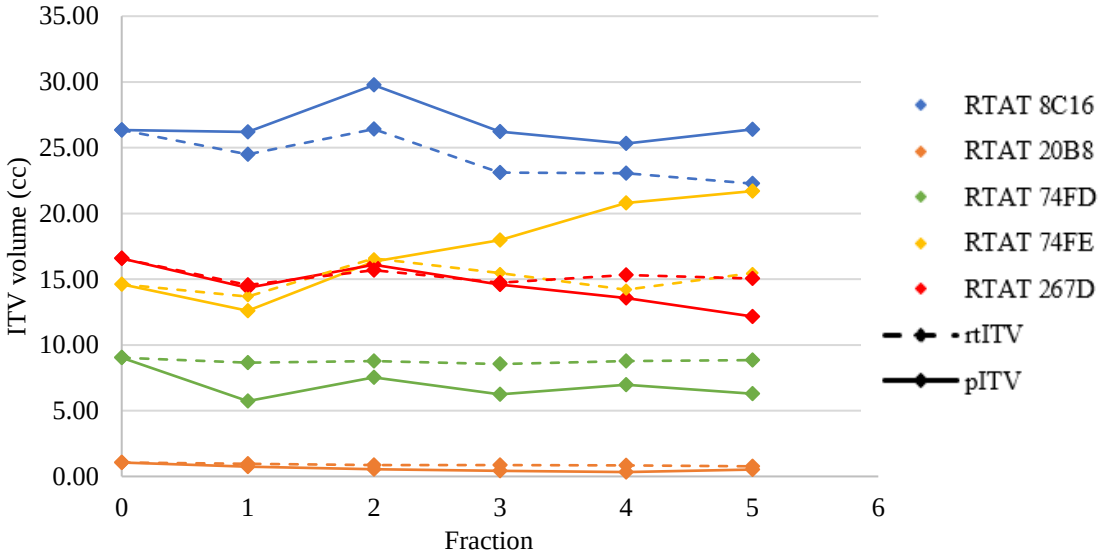

Figure 3.8: Volumes of rtITV (dashed) and pITV (solid) during treatment planning (fraction 0) and throughout the course of treatment (fraction 1 to 5) for all five patients.

Table 3.6 lists the mean values of average, 95% and maximum Hausdorff Distance (HD), and Dice coefficient (DC), comparing rtITV and pITV for the five patients. The comparison was made for all five fractions per patient independently. Overall, the mean values of average, 95%

and maximum HD, and DC were 1.44 ± 0.27 mm, 3.61 ±0.62 mm, 6.14 ± 1.24 mm, and 0.78 ± 0.03 respectively. The DC values are within 0.6 to 0.8 range, which indicates good agreement[43]. The maximum HD also indicates that the dissimilarity between rtITV and pITV was less than 1.0 cm. Figure 3.9 shows an example of the overlapping of pITV and rtITV of RTAT 267D (mean DC = 0.81, mean max HD = 4.89 mm) in fractions 3, 4 and 5. This figure shows that even though the overlapping and similarity of the two structures are good, the comparison using DC and HD is limited due to the difference in volumes of rtITV and pITV.

Table 3.6. Mean values of average, 95% and maximum HD, and dice coefficient, their corresponding standard deviation.

Patient	Ave Hausdorff distance (mm)	95% Hausdorff distance (mm)	Max Hausdorff distance (mm)	Dice coefficient
RTAT 74FE	1.76 ± 0.42	3.40 ± 0.45	8.97 ± 1.03	0.77 ± 0.04
RTAT 8C16	2.05 ± 0.25	4.43 ± 0.65	8.34 ± 1.73	0.76 ± 0.01
RTAT 267D	1.49 ± 0.41	1.98 ± 0.19	4.89 ± 1.38	0.81 ± 0.05
RTAT 20B8	0.62 ± 0.15	2.93 ± 0.83	4.81 ± 1.04	0.75 ± 0.04
RTAT 74FD	1.29 ± 0.15	3.43 ± 0.79	5.58 ± 1.21	0.79 ± 0.02

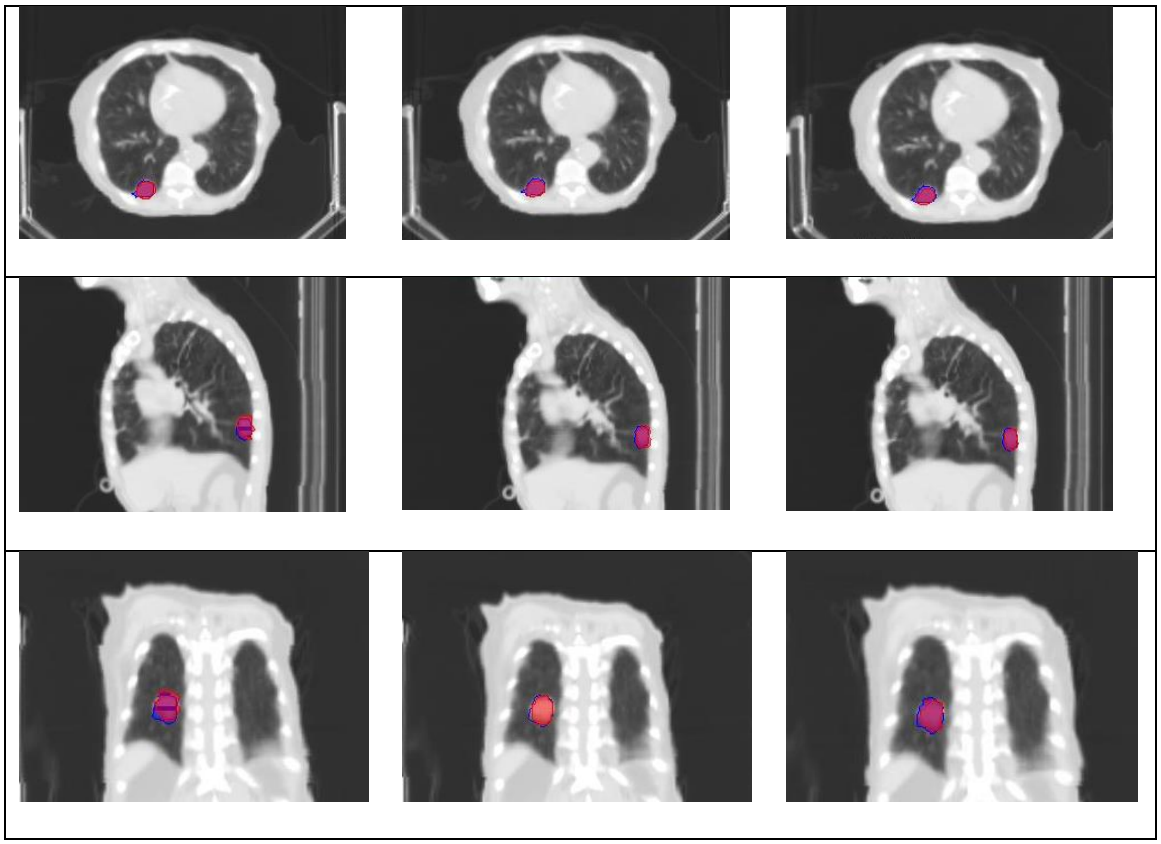

Figure 3.9: Axial, sagittal and coronal images of RTAT 267D with pITV (red) and rtITV (blue) aligned with each other in 3 fractions. From left: Fractions 3, 4, and 5.

3.3 Validation of RTapp™ dose calculation algorithm

Due to technical issues of importing studies into Pinnacle^3 for dose recalculation, five patients were omitted from this analysis. Hence, only 15 patients totaling 69 treatment fractions were used for dose recalculation. The dose metrics, which were the differences between RTapp™ predicted and Pinnacle^3 calculated values, were analyzed for every fraction. Table 3.7 lists the mean, median, and standard deviation of the dose metrics, including all 69 fractions. Positive values indicate that RTapp™ overestimates the values of the dose metrics. The dose metrics to

PTV, ITV, and GTV are underestimated by RTapp™ while the dose metrics to the OARs are overestimated.

Table 3.7. Comparison of dose metrics between RTapp™ and Pinnacle.

Dose metric	Mean	Median	Standard deviation
PTV $V_{100\%}$ (%)	-6.61	-4.32	4.57
PTV $V_{90\%}$ (%)	-1.60	-0.20	1.75
ITV $V_{100\%}$ (%)	-0.75	0.00	0.78
GTV $V_{100\%}$ (%)	-0.54	0.00	0.69
Right lung $V_{2.6Gy}$ (cc)	185.22	141.4	109.72
Left lung $V_{2.6Gy}$ (cc)	52.20	79.87	26.90
Heart $V_{6.4Gy}$ (cc)	1.10	2.25	11.79
Cord $V_{4.5Gy}$ (cc)	0.51	0.18	0.41
Esophagus $V_{5.5Gy}$ (cc)	0.27	0.19	0.78
Airway $V_{3.6Gy}$ (cc)	1.00	0.26	1.40
Right lung D_{1500cc}	0.66	0.79	0.60
Right lung D_{1000cc}	1.05	1.12	0.64
Left lung D_{1500cc}	0.44	0.29	0.52
Left lung D_{1000cc}	0.57	0.40	1.15
Heart D_{15cc}	0.73	0.26	3.00
Cord $D_{0.25cc}$	0.31	0.41	1.09
Cord $D_{0.5cc}$	-0.08	0.08	0.87
Esophagus D_{5cc}	0.65	0.40	2.22
Airway D_{4cc}	-0.55	0.00	2.21

Figure 3.10 summarizes the difference between PTV $V_{100\%}$, PTV $V_{90\%}$, ITV $V_{100\%}$, and GTV $V_{100\%}$ from RTapp™ and Pinnacle[3] for the same images with the same contour data. For the histogram plot, the differences within ± 2.5% of the categories are grouped in one bin. Out of 69 performed calculations, six shows a difference of more than 15% for PTV $V_{100\%}$. The RTapp™ reported that the target coverage values of PTV $V_{90\%}$ for 46 cases, ITV $V_{100\%}$ for 65 cases, and GTV $V_{100\%}$ for 67 cases were within 0 ± 2.5%. PTV $V_{100\%}$ values had the highest variability between RTapp™ and Pinnacle[3].

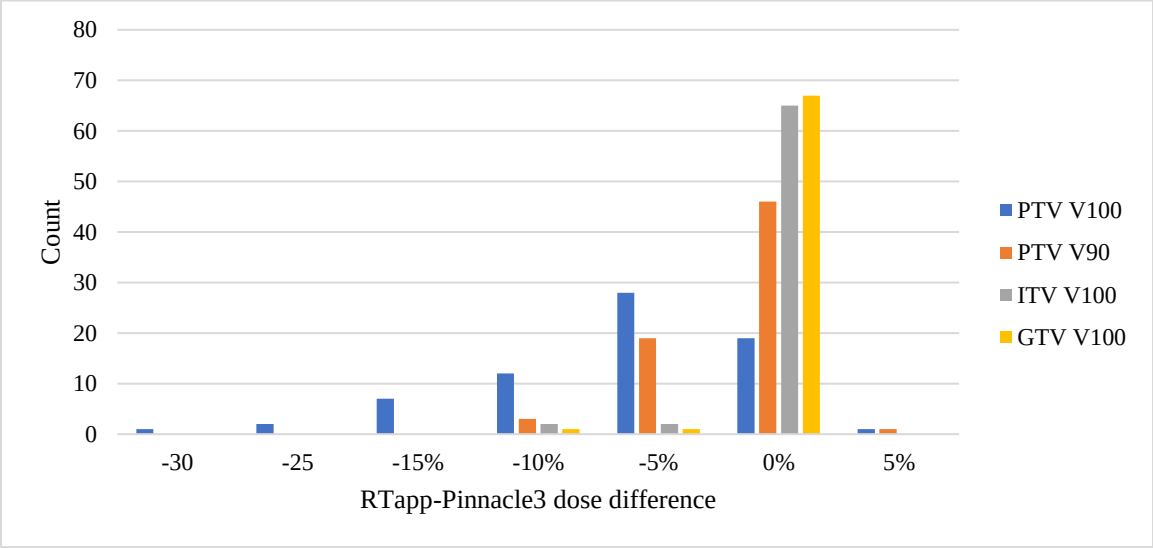

Figure 3.10: Difference between PTV $V_{100\%}$, PTV $V_{90\%}$, ITV $V_{100\%}$ and GTV $V_{100\%}$ reported in RTapp™ and Pinnacle[3].

Figure 3.11 shows the distribution of differences between RTapp™ reported OARs dose constraint and Pinnacle[3]'s OARs dose constraint. For all computed fractions, the differences of airway $V_{3.6Gy/fx}$, cord $V_{4.5Gy/fx}$, esophagus $V_{5.5Gy/fx}$ and heart $V_{6.4Gy/fx}$ were close to 0 cc with minor deviations. However, the lungs $V_{2.6Gy/fx}$ had higher variability with the maximum difference of right lung $V_{2.6Gy/fx}$ being 491.71 cc. Figure 3.12 shows the difference of predicted doses to critical volumes between RTapp™ prediction and Pinnacle[3] calculation.

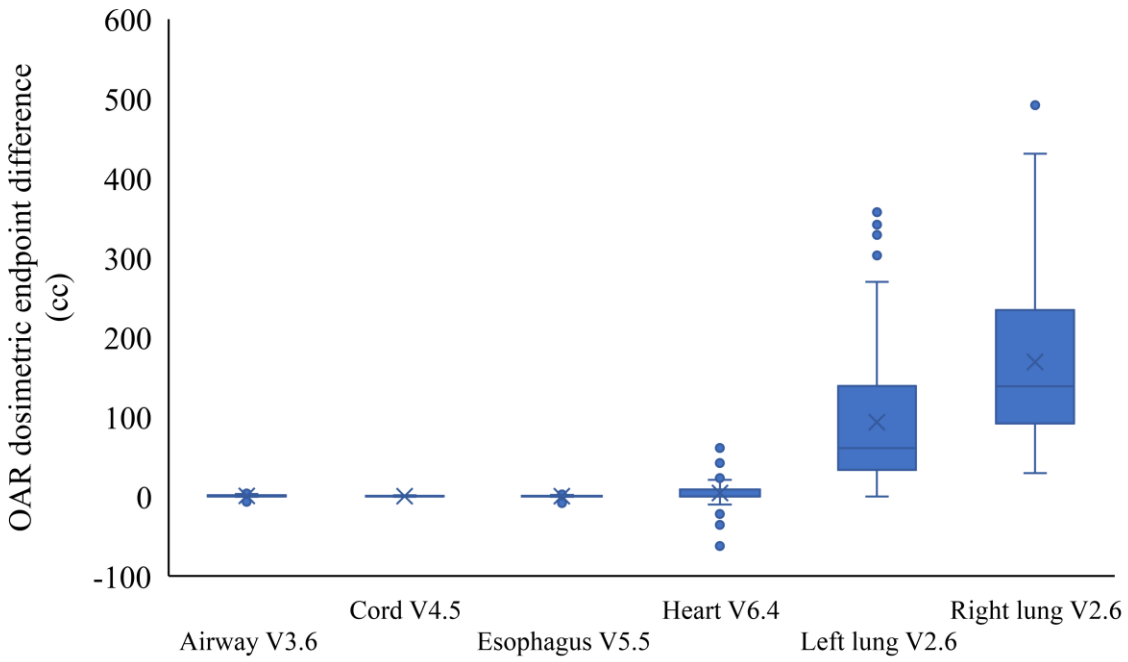

Figure 3.11: Difference between OARs dose constraints.

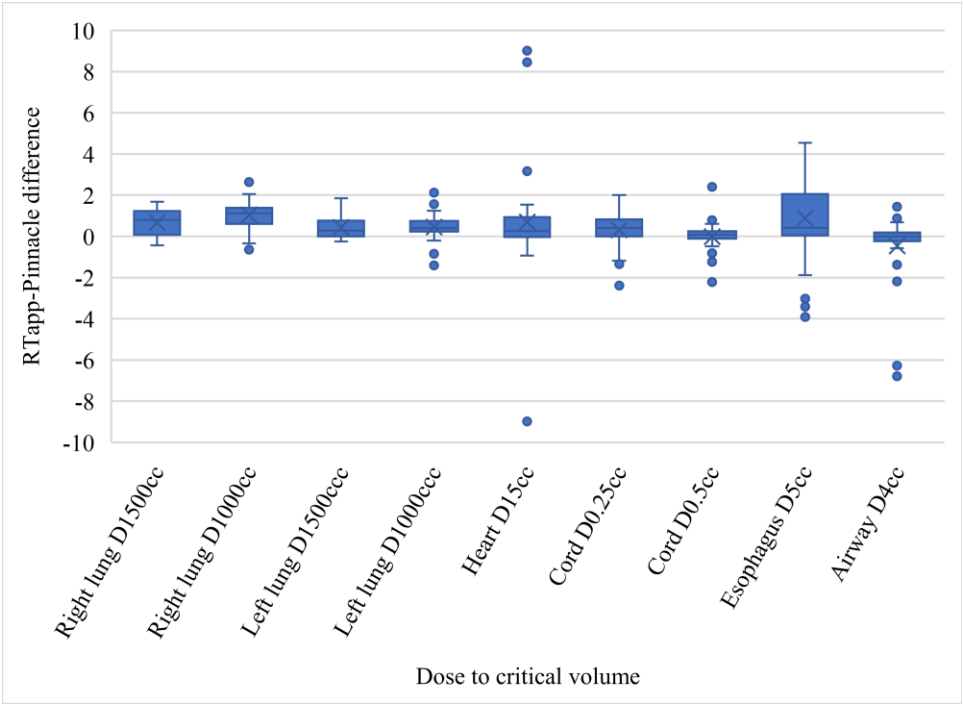

Figure 3.12. The difference between RTapp™ predicted values and Pinnacle[3] calculated values of dose to critical volumes.

The range of the difference between the dose to OAR critical volumes calculated in RTapp™ and Pinnacle^3 as shown in Figure 3.12 is between -2 Gy to 2 Gy for all dose metrics except for esophagus D_{5cc} which has a range of -2 Gy to 4 Gy. The extremities for difference of dose to critical volumes of heart, esophagus and airway belong to 3 cases and are consistent in all fractions. Case RTAT 9F44 recorded mean differences of -8.95 Gy and -3.24 Gy to 15 cc of the heart and 5 cc of the esophagus respectively. Meanwhile, case RTAT 74FE has a difference of 8.76 Gy to 15 cc of the heart and case RTAT 8C16 has a difference of -6.46 Gy to 4 cc of the airway.

4. Discussion

4.1 Summary

RTapp™ is a daily dose evaluation software that utilizes an intensity-based DIR algorithm to recontour structures and deform dose. The unique feature of RTapp™ is that it does not require a different CT density table for dose calculation. This study investigated the feasibility of RTapp™ as a daily evaluation tool by retrospectively analyzing 20 lung SBRT patients. The neutral DIR parameter was used in the evaluation of the 20 patients in RTapp™. The RTapp™ program compares daily treatment dose metric values against objectives specified during treatment planning and values recommended in RTOG protocols. A 5% review threshold was selected in all evaluations. For the current study, five patients were selected to compare the RTapp™ deformed ITV (rtITV) to physician-drawn ITV (pITV). Five patients were omitted in the dose validation process due to the technical issues of exporting the deformed CT and structures. RTapp™ calculated dose and Pinnacle^3 calculated dose were compared to assess the accuracy of the RTapp™'s DIR algorithm to update the dose distribution with the updated structures.

Current practice relies on visual inspection of the daily CBCT for the change of the tumor volume and the patient anatomy in reference to the planning image. This subjective evaluation does not address the dosimetric impact of the anatomical variations. RTapp™ not only automates structure segmentation using DIR, but it also evaluates the dosimetric effects of anatomical variations. The results of dose evaluation in RTapp™ showed the underestimation of PTV, ITV, and GTV coverages for seventeen, ten, and seven patients, respectively. There was more than a 5% decrease of PTV $V_{90\%}$ for three patients and of ITV $V_{100\%}$ and GTV $V_{100\%}$ for one patient relative to the planning values.

Furthermore, there was a negative correlation between relative volume difference and difference between planning PTV coverage values and treatment PTV coverage values. This result indicates that increased PTV volume will cause the underdosing of PTV[44]. Tatekawa et al. investigated the changes in tumor volume of lung SBRT and stated that the reduction of tumor volume adds a margin to the treatment[45]. However, in the case of RTAT 3529, the PTV was underdosed even though the tumor volume decreases. This observation confirms the importance of evaluating the dosimetric impact of anatomical variations.

4.2. PTV margin reduction by RTapp™

Figure 3.6 showed that the ITV and GTV coverage is robust against interfraction anatomical variations compared to PTV coverage shown in Figure 3.5. This is a result of the introduction of a treatment margin that accounts for the differences that can affect the tumor coverage[46]. Sun et al. stated that the interfraction variations in tumor position due to anatomical variations for lung SBRT necessitate the introduction of an additional margin for PTV[47]. RTapp™ validates the accuracy of the treatment setup by predicting the dose distribution with the daily anatomy and patient repositioning. This validation allows correction for setup errors to be performed and confirmed by ensuring the target coverage is maintained, and thus reducing the setup errors. Consequently, it is possible to reduce the setup margin with the ability to monitor the interfraction variations. The reduction of the SBRT treatment margin can alleviate toxicities and complications, especially for tumors situated close to vital organs[48,49].

4.3 Structure segmentation accuracy

In this study, the DC and HD analyses were limited to the difference in the volume of ITV of five patients. Target delineation using CBCT is susceptible to errors due to the poor quality of CBCT images[50,51]. The generation of ITV considers the internal motion of the tumor due to

respiratory motion. The longer acquisition time of CBCT produced an image of the target averaged over 12-20 breathing cycles, which is similar to planning ITV[52]. However, Liu et al. suggest that ITV drawn on CBCT is smaller than ITV drawn on 4DCT[53]. Moreover, the difference in volume also might be due to the physician's subjective judgment based on clinically meaningful information; whereas, the DIR algorithm uses only the image data or greyscale[54]. Despite the difference between rtITV and pITV, RTapp™ could generate rtITV with good agreement with pITV according to the DC and HD results. Akbarzadeh et al. categorized Dice coefficient results as follows:

- DC < 0.2 – Poor agreement
- $0.2 \leq DC \leq 0.4$ – Fair agreement
- $0.6 \leq DC \leq 0.8$ – Good agreement
- $0.8 \leq DC \leq 1.0$ – Excellent agreement

Based on this categorization, four patient's rtITVs had a good agreement with the corresponding pITVs, and one patient's rtITVs had an excellent agreement with the corresponding pITVs.

4.4. Dose calculation accuracy

In every fraction, the DVH parameters of RTapp™ were compared with those of the treatment plan. The overestimation of dose to OARs was very prominent in the lungs, notably, where the dose varied rapidly[55,56]. The effect of the high dose gradient on the dose calculation accuracy was also observed as the higher variation in PTV $V_{100\%}$. The dose outside the prescription isodose level, which conformed PTV, fell off quickly. Veiga et al. also observed larger variability in deformed dose in regions with a higher dose gradient due to uncertainties in the spatial registration[57]. The dose variations between the RTapp™ calculated dose and Pinnacle[3]

recalculated dose were also influenced by DIR uncertainties. There was a mean difference of 15.03%, 8.12%, and 5.40% for the right, left lungs, and heart, respectively. The mean difference increased for smaller structures of cord, esophagus, and airway, which were 18.43%, 21.08%, and 17.45%.

RTapp™ applies deformation to a limited portion of the planning CT, specifically to the same anatomy visualized in the CBCT. This was caused by the limited FOV size, in particular, in the superior-inferior direction, of the CBCT system. Hence, some of the structures had contours partially deformed by RTapp™. As a result, there is a truncated or displaced anatomy that influenced the dose calculation in Pinnacle^3. Figure 4.1 shows the displacement of the deformed structures compared to the normal anatomy visualized in the planning CT. This displacement might cause a specific tissue type to be displaced with different tissue density, which affected the dose distributions.

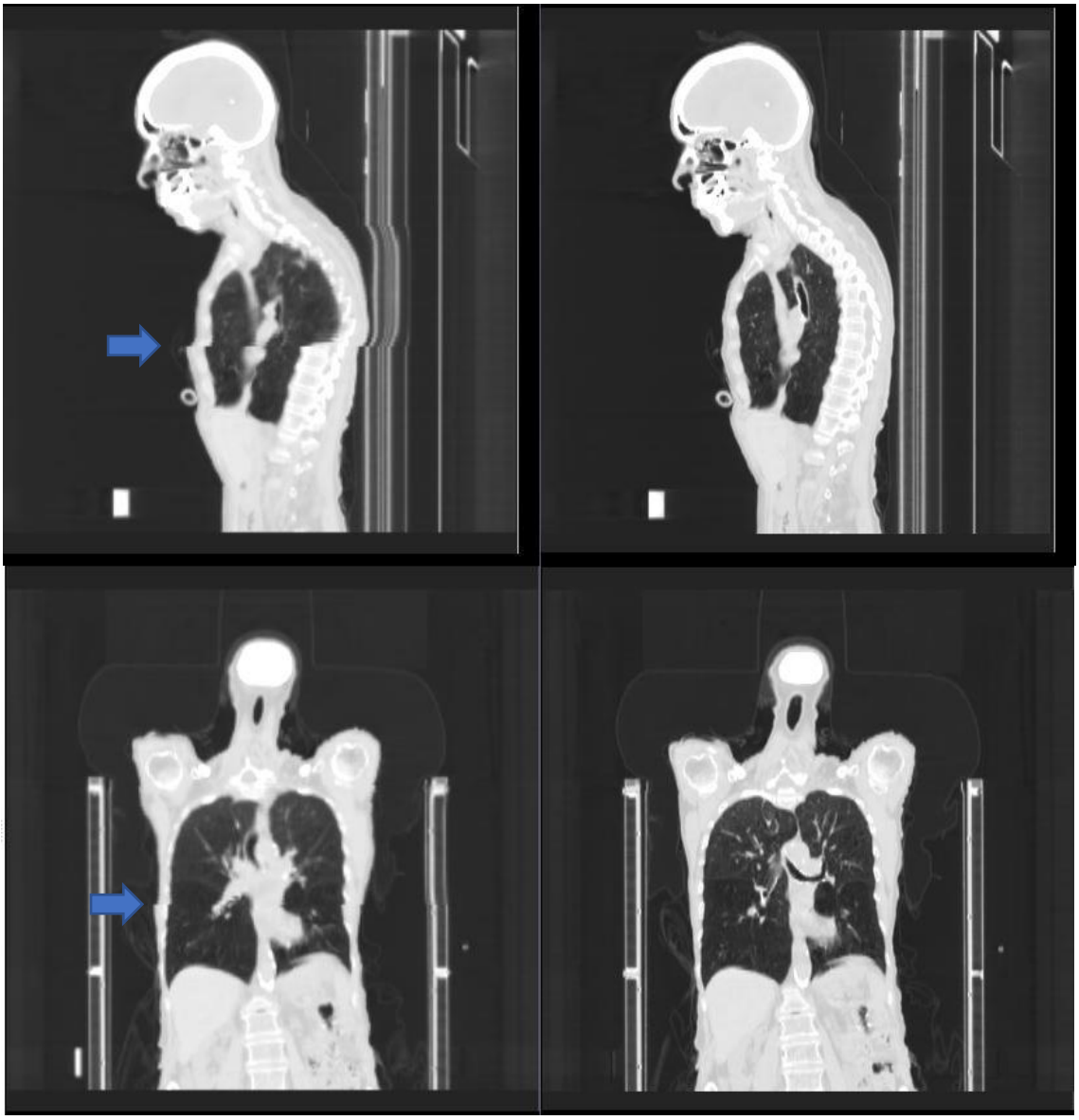

Figure 4.1. Displacement of the deformed portion of CT exported from RTapp™ and the planning CT of patient RTAT 33B6 in fraction 4.

This issue can be resolved by directly calculating the dose on CBCT if the CBCT-based HU density table is available for dose calculations[58,59]. However, Yoo et al. concluded that there is a difference between the HU density table for CBCT and CT, resulting in a dose discrepancy in both homogenous and heterogenous Catphan phantoms[60]. Yang et al. confirmed that the dose difference between CT-based dose calculation and CBCT-based dose calculation is 1% for

phantom without motion and 3% for the phantom with motion. For lung cases, a maximum of 5% dose difference was observed due to a combination of low image quality of CBCT and motion artifact[61].

4.5. DIR accuracy and reliability

It is noted that patient RTAT 74FE was aligned poorly during the patient repositioning. The images of this patient in Figure 4.2 shows the structures were displaced both in the anterior direction and in the transverse direction (to the right). This misalignment affected the accuracy of the DIR, resulting in a large volume difference between rtITV and pITV seen in Figures 3.8 and 3.9. The DIR algorithm had to increase the magnitude and direction of individual voxel distortion to align images that are further apart. However, this misalignment only resulted in more than a 5% difference in PTV coverage compared to the planning value. It did not cause GTV and ITV coverage nor the dose to OARs to be out of tolerance. It is highly advantageous if negative dosimetric impacts due to misalignment can be distinguished from effects due to other errors.

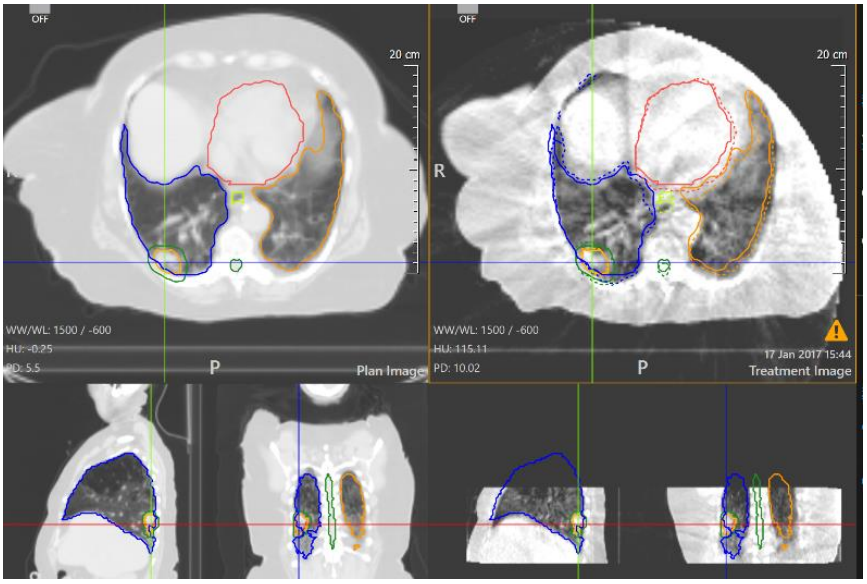

Figure 4.2. Misalignment of daily CBCT (right) of patient RTAT 74FE in fraction 5.

4.6. Shortcomings and limitations of the current analysis methods

Deformable image registration is indeed beneficial for time-efficient recontouring and dose-accumulation analysis, but it is difficult to develop validation and interpretation strategies. In addition to the DIR metrics such as HD and DC, which were used in this study, Jacobian matrices and harmonic energy analyses can provide valuable insights about the physical properties but are translated poorly to clinical understanding[62]. The volume-based dose validation methods used in this study are not efficient. The analyses, especially OAR dose validation, are oversensitive to how the DIR re-distributes the dose. The comparisons of dose parameters that represent the treatment objectives such as D_{1500cc} to lungs or D_{5cc} to esophagus confirmed the validity of RTapp™ to recognize the dose to OARs that comply with RTOG protocols. It does not analyze the accuracy of the DIR to update dose distribution. The dose metrics analyzed are in regions where dose is minimal initially; therefore, the differences are very subtle. The dose validation can be improved by analyzing the dose distributions or using the gamma analysis to evaluate the similarity of the dose distribution predicted by the DIR algorithm.

Previous literature highlighted the use of physical deformable phantoms and the virtual phantom library to validate the accuracy and to quantify the uncertainties of DIR-based contouring and dose deformation[63,64,65,66,67]. The phantoms can act as a ground truth due to the known density and volume of the structures of interest analyzed. However, it does not provide a good comparison of the heterogeneous distribution of tissues with different densities and is very unrealistic compared to clinical scenarios. The dose difference in heterogeneity might be larger in the thoracic area due to the air and bone difference, and it will be difficult to analyze such a case due to the lack of information on the uncertainty regarding respiratory motion. Another improvement that can be done is testing out-of-tolerance plans to confirm RTapp™'s ability to flag these plans as

"NOT MET". The ability of RTapp™ to detect a bad plan and how the DIR responds to plans with a large difference in tumor volumes, poor patient alignment, or images with artifacts needs to be investigated.

4.7. Expected improvement

In summary, this study indicates that further analysis is needed to investigate the reliability of RTapp™ to assist in clinical decisions by providing objective and quantitative analysis of treatment evaluation. The results of this study were obtained by using the early software release of RTapp™ (Version 1.0, 31 March 2020 update). SegAna LLC is continuously improving the RTapp™ software and will address the preliminary results in this study in the development of the software. Three areas of improvement that have been pursued since the release of the build used in this study are DIR, volume calculations, and smoothness of the contour drawing. These improvements are achieved by customizing DIR parameters so that the algorithm performs the best for specific anatomies and utilizing a fractional voxel method for volume calculations, which imitates TPS-based volume calculation, especially for structures with smaller volumes. Through these improvements, RTapp™ will be a useful daily dose evaluation tool and will benefit lung SBRT by improving the accuracy of delivered treatment.

5. Conclusions

This study aimed to investigate the feasibility of RTapp™ as a daily dose evaluation tool in adaptive lung SBRT. The preliminary results obtained using the early release of the software indicated that RTapp™ could quickly recontour structures and evaluate the dosimetric impacts of interfraction variations. It can be used to support and prompt clinical decisions to improve the quality of treatments delivered. Three patients were identified to have a decrease in PTV $V_{90\%,}$ and one patient have a decrease in ITV $V_{100\%}$ and GTV $V_{100\%}$ more than 5% of the planning values. The increase in PTV volume was found to correlate with the decrease of PTV coverage; however, one patient was predicted to have a decrease in PTV coverage despite the decrease of PTV volume. This confirms the necessity of software that, in addition to analyzing geometric variation, can analyze the dosimetric effects of anatomical changes. The ability of RTapp™'s DIR algorithm to automate contouring and update dose distribution was evaluated by using the Dice coefficient and Hausdorff distance parameters for comparisons of tumor coverage and dose metrics to OARs in Pinnacle^3 treatment planning system. The accuracy of the RTapp™ DIR algorithm should be investigated further, including comprehensive analyses of the deformed volume and dose, and how it responds to failed plans such as plans with dramatic volume change or images with an artifact.

References

1. Timmerman RD, Kavanagh BD, Cho LC, Papiez L, Xing L. Stereotactic body radiation therapy in multiple organ sites. J Clin Oncol. 2007;25(8):947-952. doi:10.1200/JCO.2006.09.7469
2. Timmerman RD. An overview of hypofractionation and introduction to this issue of seminars in radiation oncology. Semin Radiat Oncol. 2008;18(4):215-222. doi:10.1016/j.semradonc.2008.04.001
3. Benedict SH, Yenice KM, Followill D, Galvin JM, Hinson W, Kavanagh B et al. Stereotactic body radiation therapy: The report of AAPM Task Group 101. Medical physics. 2010 Aug;37(8):4078-4101. https://doi.org/10.1118/1.3438081
4. Bezjak A, Paulus R, Gaspar LE, Timmerman TD, Straube WL, Ryan WF, Garces YI, Pu AT, Singh AK, Videtic GMM, McGarry RC, Iyengar P, Pantarotto JR, Urbanic JJ, Sun AY, Daly ME, Grills IS, Sperduto P, Normolle DP, Bradley JD, Choy H. Safety and Efficacy ofa Five-Fraction Stereotactic Body Radiotherapy Schedule for Centrally Located Non-Small-Cell Lung Cancer: NRG Oncology/RTOG 0813 Trial. J Clin Oncol. 2019.
5. Khamfongkhruea C, Thongsawad S, Tannanonta C, Chamchod S. Comparison of CT images with average intensity projection, free breathing, and mid-ventilation for dose calculation in lung cancer. J Appl Clin Med Phys. 2017;18(2):26-36. doi:10.1002/acm2.12037
6. Bouilhol G, Ayadi M, Rit S, Thengumpallil S, Schaerer J, Vandemeulebroucke J, Claude L, Sarrut D. Is abdominal compression useful in lung stereotactic body radiation therapy? A 4DCT and dosimetric lobe-dependent study. European J of Med Phys. 2013;29(4):P333-340. doi:10.1016/j.ejmp.2012.04.006

7. Aznar MC, Warren S, Hoogeman M, Josipovic M. The impact of technology on the changing practice of lung SBRT. Phys Med. 2018;47:129-138. doi:10.1016/j.ejmp.2017.12.020
8. Hallemeier CL, Stauder MC, Miller RC, et al. Lung stereotactic body radiotherapy using a coplanar versus a non-coplanar beam technique: a comparison of clinical outcomes. J Radiosurg SBRT. 2013;2(3):225-233.
9. Li Y, Ma JL, Chen X, Tang FW, Zhang XZ. 4DCT and CBCT based PTV margin in Stereotactic Body Radiotherapy(SBRT) of non-small cell lung tumor adhered to chest wall or diaphragm. Radiat Oncol. 2016;11(1):152. Published 2016 15 November. doi:10.1186/s13014-016-0724-5
10. Josipovic M, Fredber Persson, Logadottir A, Smulders B, Westmann G, Peter Bangsgaard J. Translational and rotational intra- and inter-fractional errors in patient and target position during a short course of frameless stereotactic body radiotherapy. Acta Oncologica, 2012;51(5):610-617. doi: 10.3109/0284186X.2011.626448
11. Ueda, Y., Teshima, T., Cárdenes, H. and Das, I.J. Evaluation of initial setup errors of two immobilization devices for lung stereotactic body radiation therapy (SBRT). J Appl Clin Med Phys, 2017;18(4):62-68. doi:10.1002/acm2.12093
12. Belderbos J, van Beek S, van Kranen S, Rasch C, van Herk M, Sonke J. Anatomical changes during radiotherapy of lung cancer patients. Int. J Radiat Oncol Biol Phys, 2007;69(3):s508-509. doi: 10.1016/j.ijrobp.2007.07.1727
13. Wu QJ, Li T, Wu Q, Yin FF. Adaptive radiation therapy: technical components and clinical applications. Cancer J. 2011;17(3):182-189. doi:10.1097/PPO.0b013e31821da9d8

14. Lim-Reinders S, Keller BM, Al-Ward S, Saghal A, Kim A. Online Adaptive Radiation Therapy. Int. J Radiat Oncol Biol Phys, 2017;99(4):994-1003. doi:10.1016/j.ijrobp.2017.04.023
15. Yan D, Vicini F, Wong J, Martinez A. Adaptive radiation therapy. Phys Med Biol. 1997;42(1):123-132. doi:10.1088/0031-9155/42/1/008
16. Disher B, Hajdok G, Wang A, Craig J, Gaede S, Battista JJ. Correction for 'artificial' electron disequilibrium due to cone-beam CT density errors: implications for on-line adaptive stereotactic body radiation therapy of lung. Phys Med Biol. 2013;58(12):4157-4174. doi:10.1088/0031-9155/58/12/4157
17. Gomez DR, Chang JY. Adaptive radiation for lung cancer. J Oncol. 2011;2011:898391. doi:10.1155/2011/898391
18. Qin Y, Zhang F, Yoo DS, Kelsey CR, Yin FF, Cai J. Adaptive stereotactic body radiation therapy planning for lung cancer. Int J Radiat Oncol Biol Phys. 2013;87(1):209-215. doi:10.1016/j.ijrobp.2013.05.008
19. Duffton A, Harrow S, Lamb C, McJury M. An assessment of cone beam CT in the adaptive radiotherapy planning process for non-small-cell lung cancer patients. Br J Radiol. 2016;89(1062):20150492. doi:10.1259/bjr.20150492
20. Bhatt AD, El-Ghamry MN, Dunlap NE, et al. Tumor volume change with stereotactic body radiotherapy (SBRT) for early-stage lung cancer: evaluating the potential for adaptive SBRT. Am J Clin Oncol. 2015;38(1):41-46. doi:10.1097/COC.0b013e318287bd7f
21. Qin A, Gersten D, Liang J, et al. A clinical 3D/4D CBCT-based treatment dose monitoring system. J Appl Clin Med Phys. 2018;19(6):166-176. doi:10.1002/acm2.12474

22. Ma C, Cao J, Yin Y, Zhu J. Radiotherapy dose calculation on KV cone-beam CT image for lung tumor using the CIRS calibration. Thorac Cancer. 2014;5(1):68-73. doi:10.1111/1759-7714.12055
23. Kaplan LP, Elstrom UV, Moller DS, Hoffmann L. Cone beam CT based dose calculation in the thorax region. Phys and Imaging in Rad Onc. 2018;7(7):45-50. doi: 10.1016/j.phro.2018.09.001
24. Yang D, Goddu SM, Lu W, et al. Technical note: deformable image registration on partially matched images for radiotherapy applications. Med Phys. 2010;37(1):141-145. doi:10.1118/1.3267547
25. Brock KK, Mutic S, McNutt TR, Li H. and Kessler ML. Use of image registration and fusion algorithms and techniques in radiotherapy: Report of the AAPM Radiation Therapy Committee Task Group No. 132. Med. Phys. 2017;44(7): e43-e76. doi:10.1002/mp.12256
26. Jaffray DA, Lindsay PE, Brock KK, Deasy JO, Tomé WA. Accurate accumulation of dose for improved understanding of radiation effects in normal tissue. Int J Radiat Oncol Biol Phys. 2010;76(3 Suppl):S135-S139. doi:10.1016/j.ijrobp.2009.06.093
27. Yuan Z, Rong Y, Benedict SH, Daly ME, Qiu J, Yamamoto T. "Dose of the day" based on cone beam computed tomography and deformable image registration for lung cancer radiotherapy. J Appl Clin Med Phys. 2020;21(1):88-94. doi:10.1002/acm2.12793
28. RTapp™, ©SegAna LLC, FL
29. Santhanam AP, Willoughby T, Shah A, Meeks S, Rolland JP, Kupelian P. Real-time simulation of 4D lung tumor radiotherapy using a breathing model. Med Image Comput Comput Assist Interv. 2008;11(Pt 2):710-717. doi:10.1007/978-3-540-85990-1_85

30. Fedorov A, Beichel R, Kalpathy-Cramer J, et al. 3D Slicer as an image computing platform for the Quantitative Imaging Network. Magn Reson Imaging. 2012;30(9):1323-1341. doi:10.1016/j.mri.2012.05.001
31. Taha AA, Hanbury A. Metrics for evaluating 3D medical image segmentation: analysis, selection, and tool. BMC Med Imaging. 2015;15:29. Published 2015 Aug 12. doi:10.1186/s12880-015-0068-x
32. Fabri D, Zambrano V, Bhatia A, et al. A quantitative comparison of the performance of three deformable registration algorithms in radiotherapy. Z Med Phys. 2013;23(4):279-290. doi:10.1016/j.zemedi.2013.07.006
33. Hammers JE, Pirozzi S, Lindsay D, et al. Evaluation of a commercial DIR platform for contour propagation in prostate cancer patients treated with IMRT/VMAT. J Appl Clin Med Phys. 2020;21(2):14-25. doi:10.1002/acm2.12787
34. Hardcastle N, van Elmpt W, De Ruysscher D, Bzdusek K, Tomé WA. Accuracy of deformable image registration for contour propagation in adaptive lung radiotherapy. Radiat Oncol. 2013;8:243. Published 2013 18 October. doi:10.1186/1748-717X-8-243
35. Vaassen F, Hazelaar C, Vaniqui A, Gooding M, van der Heyden B, Canters R, van Elmpt W. Evaluation of measures for assessing time-saving of automatic organ-at-risk segmentation in radiotherapy. Phys and Imaging in Rad Onc. 2020;13(1):1-6. doi: 10.1016/j.phro.2019.12.001
36. Shamir RR, Duchin Y, Kim J, Sapiro G, Harel N. Continuous Dice Coefficient: a Method for Evaluating Probabilistic Segmentations. bioRxiv, 306977. 2018. doi: 10.1101/306977.

37. Zou KH, Warfield SK, Bharatha A, et al. Statistical validation of image segmentation quality based on a spatial overlap index. Acad Radiol. 2004;11(2):178-189. doi:10.1016/s1076-6332(03)00671-8
38. Dice LR. Measures of the amount of ecologic association between species. Ecology. 1945;26(3):297–302. doi: 10.2307/1932409
39. Spyridonos P, Gaitanis G, Bassukas ID, Tzaphlidou M. Gray Hausdorff distance measure for medical image comparison in dermatology: Evaluation of treatment effectiveness by image similarity. Skin Res Technol. 2013;19(1):e498-e506. doi:10.1111/srt.12001
40. Karimi D, Salcudean S. Reducing the Hausdorff Distance in Medical Image Segmentation With Convolutional Neural Networks. IEEE Transactions on Medical Imaging. 2019;39(2):499-513. doi: 10.1109/TMI.2019.2930068
41. Hausdorff_distance Class Reference. Plastimatch. Updated 8 August, 2018. Accessed 25 July, 2020. https://plastimatch.org/doxygen/classHausdorff__distance.html
42. Jani S. SU-E-J-254: Utility of Pinnacle^3 Dynamic Planning Module Utilizing Deformable Image Registration in Adaptive Radiotherapy. Med Phys. 2014;41(6):216. doi: 10.1118/1.4888308
43. Akbarzadeh A, Gutierrez D, Baskin A, et al. Evaluation of whole-body MR to CT deformable image registration. J Appl Clin Med Phys. 2013;14(4):4163. Published 2013 Jul 8. doi:10.1120/jacmp.v14i4.4163
44. Parker SM, Siochi RA, Wen S, Mattes MD. Impact of Tumor Size on Local Control and Pneumonitis After Stereotactic Body Radiation Therapy for Lung Tumors. Pract Radiat Oncol. 2019;9(1):e90-e97. doi:10.1016/j.prro.2018.09.003

45. Tatekawa K, Iwata H, Kawaguchi T, Ishikura S, Baba F, Otsuka S, Miyakawa A, Iwana M, Shibamoto Y. Changes in volume of stage I non-small-cell lung cancer during stereotactic body radiotherapy. Radiat Oncol. 2014;9(1):8. doi:10.1186/1748-717X-9-8
46. Shah C, Kestin LL, Hope AJ, et al. Required target margins for image-guided lung SBRT: Assessment of target position intrafraction and correction residuals. Pract Radiat Oncol. 2013;3(1):67-73. doi:10.1016/j.prro.2012.03.004
47. Sun Y, Lu Y, Cheng S, et al. Interfractional variations of tumor centroid position and tumor regression during stereotactic body radiotherapy for lung tumor. Biomed Res Int. 2014;2014:372738. doi:10.1155/2014/372738
48. Navran A, Heemsbergen W, Janssen T, et al. The impact of margin reduction on outcome and toxicity in head and neck cancer patients treated with image-guided volumetric modulated arc therapy (VMAT). Radiother Oncol. 2019;130:25-31. doi:10.1016/j.radonc.2018.06.032
49. Kang KH, Okoye CC, Patel RB, et al. Complications from Stereotactic Body Radiotherapy for Lung Cancer. Cancers (Basel). 2015;7(2):981-1004. Published 2015 15 June. doi:10.3390/cancers7020820
50. Segedin B, Petric P. Uncertainties in target volume delineation in radiotherapy - are they relevant and what can we do about them?. Radiol Oncol. 2016;50(3):254-262. Published 2016 9 May. doi:10.1515/raon-2016-0023
51. Thengumpallil, S., Smith, K., Monnin, P., Bourhis, J., Bochud, F. and Moeckli, R. (2016), difference in performance between 3D and 4D CBCT for lung imaging: a dose and image quality analysis. Journal of Applied Clinical Medical Physics, 17: 97-106. doi:10.1120/jacmp.v17i6.6459

52. Vergalasova I, Maurer J, Yin FF. Potential underestimation of the internal target volume (ITV) from free-breathing CBCT. Med Phys. 2011;38(8):4689-4699. doi:10.1118/1.3613153

53. Liu HW, Khan R, D'Ambrosi R, Krobutschek K, Nugent Z, Lau H. The influence of target and patient characteristics on the volume obtained from cone beam CT in lung stereotactic body radiation therapy. Radiother Oncol. 2013;106(3):312-316. doi:10.1016/j.radonc.2013.01.001

54. Whitfield GA, Price P, Price GJ, Moore CJ. Automated delineation of radiotherapy volumes: are we going in the right direction?. Br J Radiol. 2013;86(1021):20110718. doi:10.1259/bjr.20110718

55. Roussakis YG, Dehghani H, Green S, Webster GJ. Validation of a dose warping algorithm using clinically realistic scenarios. Br J Radiol. 2015;88(1049):20140691. doi:10.1259/bjr.20140691

56. Tilly D, Tilly N, Ahnesjö A. Dose mapping sensitivity to deformable registration uncertainties in fractionated radiotherapy - applied to prostate proton treatments. BMC Med Phys. 2013;13(1):2. Published 2013 14 June. doi:10.1186/1756-6649-13-2

57. Veiga C, McClelland J, Moinuddin S, et al. Toward adaptive radiotherapy for head and neck patients: Feasibility study on using CT-to-CBCT deformable registration for "dose of the day" calculations. Med Phys. 2014;41(3):031703. doi:10.1118/1.4864240

58. Barateau A, Garlopeau C, Cugny A, et al. Dose calculation accuracy of different image value to density tables for cone-beam CT planning in head & neck and pelvic localizations. Phys Med. 2015;31(2):146-151. doi:10.1016/j.ejmp.2014.12.007

59. Chen S, Le Q, Mutaf Y, et al. Feasibility of CBCT-based dose with a patient-specific stepwise HU-to-density curve to determine time of replanning. J Appl Clin Med Phys. 2017;18(5):64-69. doi:10.1002/acm2.12127
60. Yoo S, Yin FF: Dosimetric feasibility of cone-beam CT-based treatment planning compared to CT-based treatment planning. Int J Radiat Oncol Biol Phys 2006, 66: 1553-1561.
61. Yang Y, Schreibmann E, Li T, et al.: Evaluation of on-board kV cone beam CT (CBCT)-based dose calculation. Phys Med Biol 2007, 52: 685-705. 10.1088/0031-9155/52/3/011
62. Paganelli C, Meschini G, Molinelli S, Riboldi M, Baroni G. "Patient-specific validation of deformable image registration in radiation therapy: Overview and caveats". Med Phys. 2018;45(10):e908-e922. doi:10.1002/mp.13162
63. Liao Y, Wang L, Xu X, et al. An anthropomorphic abdominal phantom for deformable image registration accuracy validation in adaptive radiation therapy. Med Phys. 2017;44(6):2369-2378. doi:10.1002/mp.12229
64. Matrosic CK, Hull J, Palmer B, Culberson W, Bednarz B. Deformable abdominal phantom for the validation of real-time image guidance and deformable dose accumulation. J Appl Clin Med Phys. 2019;20(8):122-133. doi:10.1002/acm2.12687
65. Kashani R, Hub M, Kessler ML, Balter JM. Technical note: a physical phantom for assessment of accuracy of deformable alignment algorithms. Med Phys. 2007;34(7):2785-2788. doi:10.1118/1.2739812
66. Kim H, Park SB, Monroe JI, et al. Quantitative Analysis Tools and Digital Phantoms for Deformable Image Registration Quality Assurance. Technol Cancer Res Treat. 2015;14(4):428-439. doi:10.1177/1533034614553891

67. Pukala J, Meeks SL, Staton RJ, Bova FJ, Mañon RR, Langen KM. A virtual phantom library for the quantification of deformable image registration uncertainties in patients with cancers of the head and neck. Med Phys. 2013;40(11):111703. doi:10.1118/1.4823467